A MOLECULAR-FIELD APPROXIMATION FOR QUANTUM CRYSTALS

by Ronald L. Danilowicz

N75-18351

(NASA-CR-142316) A MOLECULAR-FIELD APPROXIMATION FOR QUANTUM CRYSTALS Ph.D. Thesis (Colorado State Univ.) 63 p HC $3.75 CSCL 20B

Unclas
G3/25 13519

Department of Physics

Colorado State University

Fort Collins, Colorado

THESIS

A MOLECULAR-FIELD APPROXIMATION FOR QUANTUM CRYSTALS

Submitted by

Ronald L. Danilowicz

In partial fulfillment of the requirements

for the Degree of Doctor of Philosophy

Colorado State University

Fort Collins, Colorado

May, 1973

COLORADO STATE UNIVERSITY

WE HEREBY RECOMMEND THAT THE THESIS PREPARED UNDER OUR SUPERVISION BY Ronald L. Danilowicz ENTITLED A MOLECULAR-FIELD APPROXIMATION FOR QUANTUM CRYSTALS BE ACCEPTED AS FULFILLING IN PART REQUIREMENTS FOR THE DEGREE OF Doctor of Philosophy.

Committee on Graduate Work

Adviser

Head of Department

ABSTRACT OF THESIS

A MOLECULAR-FIELD APPROXIMATION FOR QUANTUM CRYSTALS

Ground-state properties of quantum crystals have received considerable attention from both theorists and experimentalists. The theoretical results have varied widely with the Monte Carlo calculations being the most successful. The molecular field approximation yields ground-state properties which agree closely with the Monte Carlo results. This approach evaluates the dynamical behavior of each --ir of molecules in the molecular field of the other N-2 molecules. In addition to predicting ground-state properties that agree well with experiment, this approach yields interesting data on the relative importance of interactions of different nearest neighbor pairs. Results are presented for b.c.c. He^3 and b.c.c. He^4 at low and high densities (down to 10 cm^3/mole). Results are also presented for f.c.c. H_2 over a similar density range.

Ronald Leonard Danilowicz
Physics Department
Colorado State University
Fort Collins, Colorado 80521
May, 1973

ACKNOWLEDGMENTS

I wish to acknowledge the guidance and friendship of my adviser, Dr. Richard D. Etters, throughout the course of this study. It is a pleasure to thank the other members of my committee, Professor John C. Raich, Sanford Kern, and Carl W. Wilmsen.

The author is grateful for the financial assistance of the National Aeronautics and Space Administration and for the interest of Miss G. Collins and the Training Committee.

Finally, I wish to thank my wife, Lucy, and my two children for their patience and understanding.

TABLE OF CONTENTS

LIST OF TABLES

LIST OF FIGURES

I. INTRODUCTION

There have been a number of theoretical investigations of the ground-state properties of quantum crystals over the last decade. A quantum crystal is one in which the zero point excursion of a molecule from its equilibrium lattice position is a large fraction of the nearest neighbor distance. This is in contrast to most crystals where the amplitude of the oscillations about the equilibrium position is small compared to the interatomic spacing at low temperature. This allows the dynamics of most crystals to be described classically in terms of a collection of harmonic oscillators.

The large oscillations in quantum crystals, a result of small atomic mass and the weakness of the attractive part of the interaction potential, invalidate the typical classical approach necessitating the use of quantum mechanics for their description. In the treatment of quantum crystals, another important consequence of the large zero point motion must be properly accounted for. This is the strong correlation of the motion of neighboring pairs of molecules. The relative motion of neighboring pairs is correlated in such a way as to avoid close encounters which involve the strong short-range repulsive forces.

Most of the recent published calculations employ a variational technique with trial wave functions which contain short-range correlations. The variational approach relies on the Rayleigh-Ritz variational principle given by

$$E_o \leq \frac{\langle\psi|H|\psi\rangle}{\langle\psi|\psi\rangle} \qquad (1)$$

where E_o is the ground state energy, H is the Hamiltonian of the system, and $|\psi\rangle$ is an approximation to the ground state wave function, $|\psi_o\rangle$. A complete list of symbols appears in Appendix A. The right-hand side of equation (1) represents an upper bound to the ground state energy which approaches E_o as $|\psi\rangle$ approaches $|\psi_o\rangle$ with equality when $|\psi\rangle = |\psi_o\rangle$.

A simple form for the N-particle wave function which contains short-range correlations was first introduced by Jastrow.[1] It is

$$\psi(\bar{r}_1,\bar{r}_2,\ldots\bar{r}_N) = \prod_{i=1}^{N} \phi(\bar{r}_i) \prod_{j<\kappa}^{N} f(r_{j\kappa}), \qquad r_{j\kappa} = |\bar{r}_j - \bar{r}_\kappa| \qquad (2)$$

where $\phi(\bar{r}_i)$ is a single particle wave function centered about the equilibrium lattice position $\bar{R}_i$ and the $f(r_{j\kappa})$ are $\frac{N}{2}(N-1)$ spherically symmetric two-body correlation functions. The limiting behavior for the two-body correlation functions is $\lim_{r\to 0} f(r) = 0$ and $\lim_{r\to\infty} f(r) = 1$. Therefore, the $f(r)$ functions lower the probability of finding two molecules close together while having no effect at large distances.

The N-particle Hamiltonian is given by

$$H = -\frac{h^2}{2m}\sum_{\kappa=1}^{N}\nabla_\kappa^2 + \frac{1}{2}\sum_{i\neq j}^{N}\sum_{j=1}^{N}\nu(r_{ij}) \qquad (3)$$

where $\nu(r_{ij})$ represents the interatomic potential between the i^{th} and j^{th} molecules. Evaluation of the right-hand side of equation (1) therefore involves the calculation of on the order of N^2 integrals all containing 3N dimensions. The differences in the recent theories are a result of the manner in which each one evaluates this expression.

The first technique used with much success was the work of Nosanow[2] which employed the use of a cluster expansion similar to those used in statistical mechanics. Similar cluster expansion techniques have been employed in much of the work on quantum crystals.[3-10] A slightly different expansion has been used by Guyer.[11] He and Werthamer have each written review articles which cover most of the material mentioned above.[12,13] More recently, Horner[14] has formulated a perturbation theory of quantum crystals.

Most of these formulations give only fair agreement with experimental data. The cluster expansions, however, converge rapidly enough to be useful only for a very limited set of two-body correlation functions. They require $f(r)$ to approach rapidly its limiting value of unity. A satisfactory set of correlation functions at low densities may be unsatisfactory at high pressures when the nearest neighbor distance becomes smaller. An additional problem is that in a cluster expansion the completely free variation of both the single particle wave functions and the two body correlation functions leads to a liquid solution. This is discussed in detail in Guyer's review article.[12]

An approach which avoids these difficulties and also comes closest to matching experimental data is the Monte Carlo representation used by Hansen and coworkers.[15-19] Most differences that remain with experiment are attributed primarily to an inadequate representation for the two-body interaction potential, $\nu(r)$.

The work presented here is an important improvement over the use of a cluster expansion. It also removes the restrictions on the two-body correlation functions necessary for good convergence of the cluster expansion. This approach evaluates the dynamical behavior of each pair of molecules in the molecular field of the other $N - 2$ molecules. It is found necessary to incorporate in the molecular field the approximate motion of the nearest neighbors to the dynamic pair. This molecular field approximation gives results for He^3 and He^4 which agree closely with experiment and the results from the Monte Carlo representation. As in the recent investigation by Hansen[19] the range of density covered has been extended to higher densities (10 cm^3/mole) where the cluster expansions used to date are invalid.

Results are also presented for solid molecular hydrogen. In addition to predicting ground-state properties that agree well with experiment for both H_2, He^3 and He^4, this approach yields data on the importance of interactions of different nearest neighbor pairs, and data showing the effects of dynamic motion.

II. MOLECULAR FIELD THEORY

The expectation value for the Hamiltonian for an N-particle system is

$$\langle H\rangle = \langle\psi|\psi\rangle^{-1}\langle\psi| -\frac{\hbar^2}{2m}\sum_{\kappa=1}^{N}\nabla_\kappa^2 + \frac{1}{2}\sum_{i\neq j}^{N}\sum_{j=1}^{N} v(r_{ij})|\psi\rangle \tag{4}$$

where the wave function $|\psi\rangle$ is of the form given by equation (2). At this point it is convenient to introduce a procedure first noted by Jackson and Feenberg.[20] The expectation value of a typical term in the kinetic energy is

$$\langle\psi| -\frac{\hbar^2}{2m}\nabla_\kappa^2|\psi\rangle = -\frac{\hbar^2}{2m}\int \psi^* \nabla_\kappa^2\psi \, d\bar{r}_1 \, d\bar{r}_2 \, . \, . \, . \, d\bar{r}_N \tag{5}$$

Using Green's Theorem

$$\int \psi^* \nabla^2\psi \, \overline{dr}_1 \, \overline{dr}_2 \, . \, . \, . \, \overline{dr}_N = -\int \bar{\nabla}\psi^* \cdot \bar{\nabla}\psi \, \overline{dr}_1 \, \overline{dr}_2 \, . \, . \, . \, \overline{dr}_N \tag{6}$$

Therefore equation (5) can be rewritten as

$$-\frac{\hbar^2}{4m}\int \left(\psi^*\nabla_\kappa^2\psi - \bar{\nabla}_\kappa\psi^* \cdot \bar{\nabla}_\kappa\psi\right)\overline{dr}_1 \, \overline{dr}_2 \, . \, . \, . \, \overline{dr}_N \tag{7}$$

If we allow ψ to be only real then equation (7) becomes

$$-\frac{\hbar^2}{4m}\int \psi^2 \, \nabla_\kappa^2 \ln\psi \, \overline{dr}_1 \, \overline{dr}_2 \, . \, . \, . \, \overline{dr}_N \tag{8}$$

by virtue of

$$\nabla^2 \ln\psi = \frac{1}{\psi}\nabla^2\psi - \frac{1}{\psi^2}(\nabla\psi)^2 \tag{9}$$

Using a ψ of the form given by equation (2) gives finally

$$-\frac{\hbar^2}{4m}\int \psi^2\left[\nabla_\kappa^2 \ln\phi(\bar{r}_\kappa) + \sum_{\kappa\neq j}^{N} \nabla_\kappa^2 \ln f(r_{\kappa j})\right]\overline{dr}_1\,\overline{dr}_2\,.\,.\,.\,\overline{dr}_N \tag{10}$$

We can now rewrite equation (4) as

$$\langle H\rangle = \left\{\int \psi^2\left[\sum_{\kappa=1}^{N} -\frac{\hbar^2}{4m}\nabla_\kappa^2 \ln\phi(\bar{r}_\kappa) + \frac{1}{2}\sum_{i\neq j}^{N}\sum_{j=1}^{N} V_{ij}\right]\overline{dr}_1\,.\,.\,.\,\overline{dr}_N\right\}$$

$$* \left\{\int \psi^2\,\overline{dr}_1\,\overline{dr}_2\,.\,.\,.\,\overline{dr}_N\right\}^{-1} \tag{11}$$

with

$$V_{ij} \equiv v(r_{ij}) - \frac{\hbar^2}{2m}\nabla_{ij}^2 \ln f(r_{ij}) \tag{12}$$

A common choice for the form of the single particle wave function $\phi(\bar{r}_\kappa)$ is

$$\phi(\bar{r}_\kappa) = \left(\frac{\beta}{\pi}\right)^{3/4} \exp\left[-\frac{\beta}{2}(\bar{r}_\kappa - \bar{R}_\kappa)^2\right] \tag{13}$$

with this form

$$\nabla_\kappa^2 \ln\phi(\bar{r}_\kappa) = -3\beta$$

and equation (11) further simplifies to

$$\langle H\rangle = \frac{3N\hbar^2\beta}{4m} + \left[\int \frac{\psi^2}{2}\sum_{i\neq j}^{N}\sum_{j=1}^{N} V_{ij}\,\overline{dr}_1\,.\,.\,.\,\overline{dr}_N\right]$$

$$\left[\int \psi^2\,\overline{dr}_1\,.\,.\,.\,\overline{dr}_N\right]^{-1} \tag{14}$$

and the expectation value per particle is just

$$\frac{\langle H\rangle}{N} = \frac{3\hbar^2\beta}{4m} + \left\{\int \frac{\psi^2}{2} \sum_{i\neq j}^{N} V_{ij}\, \overline{dr}_1 \ldots \overline{dr}_N\right\}\left\{\int \psi^2\, \overline{dr}_1 \ldots \overline{dr}_N\right\}^{-1} \tag{15}$$

It is at this point that the recent theories for quantum crystals diverge. Each solves this equation in a different manner for various parameterized forms of the two-body correlation function, $f(r)$. In the static molecular field theory approximation the effective molecular field acting on an arbitrary pair is found by assuming that the $N - 2$ other molecules are fixed at their respective equilibrium lattice positions. This is accomplished by letting the λth and κth molecules represent the arbitrary pair and by taking the limit $\phi^2(\overline{r}_i - \overline{R}_i) \to \delta(\overline{r}_i - \overline{R}_i)$ for all other $N - 2$ molecules (i.e., $i \neq \lambda,\kappa$).

Neglecting the constant in equation (15) we can arrange the remainder so that the sum is of contributions to the energy from successive nearest neighbor shells. Rewriting equation (15) in this manner gives

$$\frac{\langle H\rangle}{N} = \frac{3\hbar^2\beta}{4m} + \frac{1}{2}\left\{N_1\left(\frac{\int \psi^2 V_{\lambda\kappa}\, \overline{dr}_1 \ldots \overline{dr}_N}{\int \psi^2\, \overline{dr}_1 \ldots \overline{dr}_N}\right)_{(\lambda,\kappa)\text{1st n.n.}} + N_2\left(\frac{\int \psi^2 V_{\lambda\kappa}\, \overline{dr}_1 \ldots \overline{dr}_N}{\int \psi^2\, \overline{dr}_1 \ldots \overline{dr}_N}\right)_{(\lambda,\kappa)\text{2nd n.n.}} + \ldots\right\} \tag{16}$$

where the N_i's are the number of neighbors in each shell and (λ,κ) 1st n.n. means the λth and κth molecules are first nearest neighbors, etc. By letting $\phi(\overline{r}_i - \overline{R}_i) \to \delta(\overline{r}_i - \overline{R}_i)$ in this expression for all $i \neq \lambda,\kappa$ we get

$$\frac{\langle H\rangle}{N} = \frac{3\hbar^2\beta}{4m} + \frac{N_1}{2}\left(\frac{\int \phi^2(\bar{r}_\kappa - \bar{R}_\kappa)\,\phi^2(\bar{r}_\lambda - \bar{R}_\lambda)\, f^2(\bar{r}_{\lambda\kappa}) \prod\limits_{s\neq\lambda,\kappa} f^2(\bar{r}_\kappa - \bar{R}_s) \prod\limits_{\rho\neq\lambda,\kappa} f^2(\bar{r}_\lambda - \bar{R}_\rho)\, V_{\lambda\kappa}\, \overline{dr}_\lambda\, \overline{dr}_\kappa}{\int \phi^2(\bar{r}_\kappa - \bar{R}_\kappa)\,\phi^2(\bar{r}_\lambda - \bar{R}_\lambda)\, f^2(\bar{r}_{\lambda\kappa}) \prod\limits_{s\neq\lambda,\kappa} f^2(\bar{r}_\kappa - \bar{R}_s) \prod\limits_{\rho\neq\lambda,\kappa} f^2(\bar{r}_\lambda - \bar{R}_\rho)\, \overline{dr}_\lambda\, \overline{dr}_\kappa}\right)_{(\lambda,\kappa)\,\mathrm{1st\ n.n.}} + \ldots \qquad (17)$$

In a previous paper[21] this expression was further simplified by assuming that the products over s and ρ to first order need only be carried out over first nearest neighbors to λ and κ. Each function $f^2(\bar{r}_\kappa - \bar{R}_s)$ was then expanded about its value evaluated at the equilibrium lattice site separation, $f^2(\bar{R}_\kappa - \bar{R}_s)$. These were angle averaged and reduced equation (17) to a collection of easily solvable two-dimensional integrals.

Recently equation (17) has been evaluated more exactly by calculating the six-dimensional integrals numerically using Monte Carlo techniques. The products of two-body correlation functions in equation (17) contain all of the correlation functions which couple the λth and κth molecules to every other molecule in the system. In practice this product was only extended over the first three nearest neighbor shells of the λth and κth molecules. For the two-body correlation function considered in this investigation, this was an adequate representation. The values for $f^2(\overline{r}_\kappa - \overline{R}_s)$ and $f^2(\overline{r}_\lambda - \overline{R}_\rho)$ outside of this range were unity. This approximation is easily changed and can be adjusted to include more nearest neighbor shells as the two-body correlation functions considered become more long ranged.

Also, the terms in equation (17) extend over the entire lattice. In practice only the contributions from the first ten nearest neighbor shells are calculated exactly. The contributions from the remaining shells are evaluated for a static lattice. This is a more than adequate approximation. In the Monte Carlo calculations mentioned previously[15-19] only the first four nearest neighbor shells are evaluated exactly. The details of the evaluation of equation (17) can be found in Appendix B.

The forms of trial wave function and interaction potential used in this study are primarily those that have received the most attention in other studies. This is because the intent at this point is a comparison of techniques for evaluating equation (1) rather than a detailed study of various trial wave functions and interaction potentials. The trial wave functions used in this study therefore are in the form given by equation (2). The single particle wave functions in that equation are given for this study by equation (13). The two-body correlation function used is the one which corresponds to the WKB solution of the two-body Schrödinger equation with a Lennard-Jones potential in the limit as $r_{ij} \to 0$. It has the form

$$f(r_{ij}) = \exp\left\{-\frac{1}{2}\left(\frac{\kappa}{r_{ij}}\right)^5\right\} \tag{18}$$

Finally the interaction potentials used for this study were of the Lennard-Jones type given by

$$\nu(r_{ij}) = 4\varepsilon\left[\left(\frac{\sigma}{r_{ij}}\right)^{12} - \left(\frac{\sigma}{r_{ij}}\right)^{6}\right] \tag{19}$$

where $\varepsilon = 10.22^\circ$ K, $\sigma = 2.556$ Å for helium, and $\varepsilon = 37^\circ$ K, $\sigma = 2.93$ Å for hydrogen.

III. RESULTS AND DISCUSSION

Equation (17) was evaluated using standard Monte Carlo integration techniques[22] for a wide range of variables. The results for He^4, He^3, and H_2 were somewhat disappointing. In each case the ground-state energy at zero pressure agreed quite well with experiment. However, in each case this minimum with respect to our two variational parameters, β and κ, occurred for a value of $\beta = 0$. The corresponding value for κ was also higher than the value given by investigators using random walk Monte Carlo techniques. These results at zero pressure alone were not completely surprising since this is near the liquid-solid transition. Also, as has been pointed out by other investigators,[15,19] the ground-state energy is a slowly varying function of the variational parameters in the vicinity of the minima. This was the case in this study as the value of E_o at $\beta = 0$ was not much less than the value obtained for the minimizing values of β and κ reported elsewhere. However, the disturbing part of the results was the fact that the minimum with respect to β was at $\beta = 0$ for all densities. Even though this corresponds to a solid in our calculation unlike the cluster expansion, it resulted in a trial wave function with effectively only one variational parameter, which was undesirable. The resulting ground-state energies dropped increasingly below experimental values for increasing densities. Typical results for He^4 are shown in figure 1.

A. New Formalism

It was felt that these poor results were due to the rigidity of the surrounding lattice. The localizing of molecules on individual

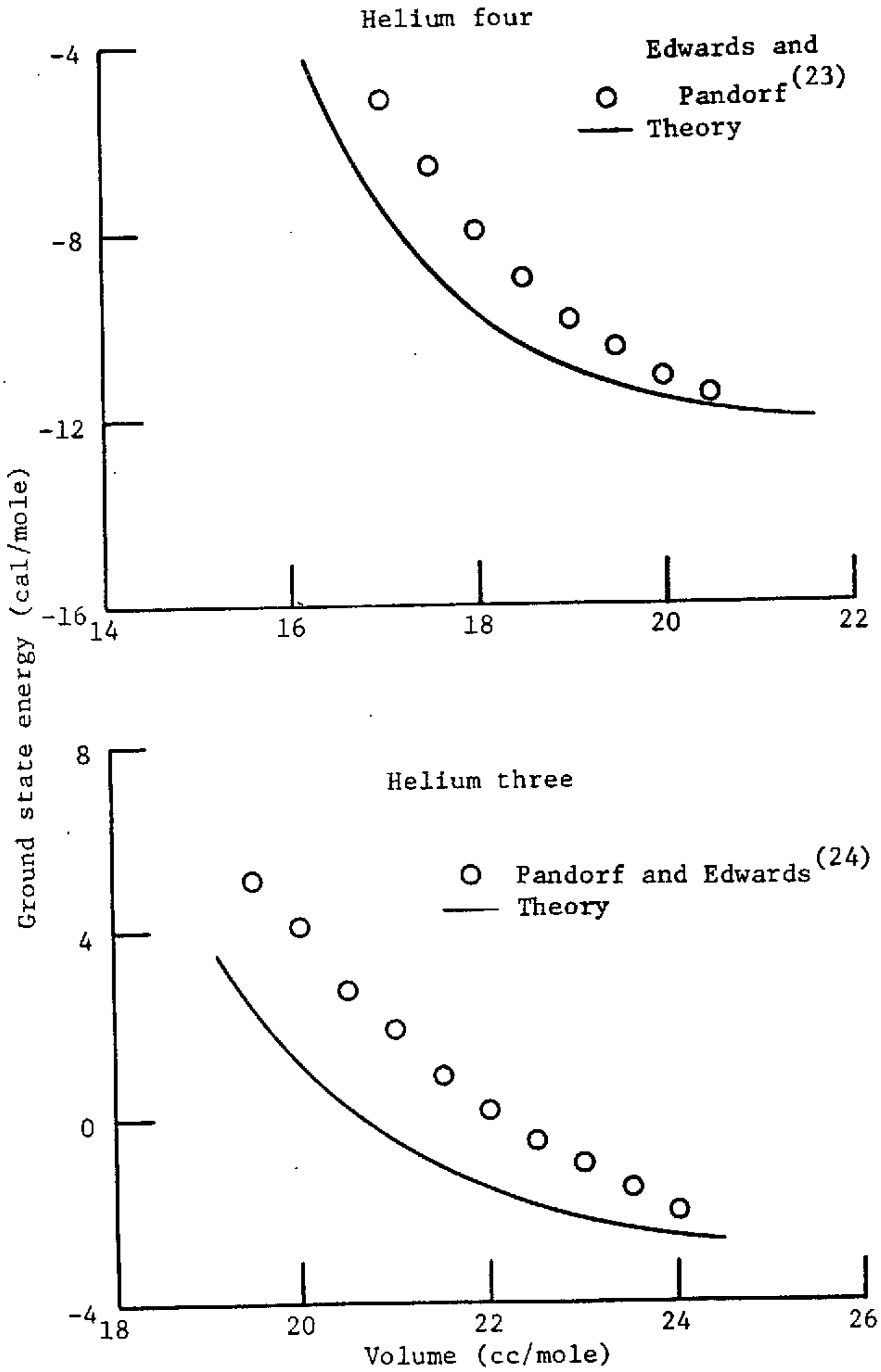

Figure 1. Results with six-dimensional formalism.

lattice sites comes partially from the single particle wave functions and partially from the two-body correlation functions. With surrounding molecules fixed on their respective lattice sites, a molecule was confined to a smaller volume than it would have been if these molecules were allowed to move. This is another way of saying that the correlations with the surrounding lattice were doing more than their proper share of the localizing. This in turn allowed the single particle wave functions to spread out.

MacMahan[25] calculates the exchange integral for He^3, J, using a Monte Carlo calculation and also by evaluating the six-dimensional integral obtained by fixing all but the exchanging pair of atoms on their equilibrium lattice sites similar to our approach for the ground-state energy. He finds good agreement at zero pressure for the two techniques but the results rapidly diverge as the pressure increases. He concludes as we do that the rigidity of the lattice is to blame and this effect is more pronounced at higher densities.

The solution is then to allow in some approximate fashion some movement of the surrounding lattice. It was felt that allowing the motion of the nearest neighbors of each of the molecules in the dynamic pair (λ,κ) would be sufficient to remove the difficulties with the results. This was verified by later results.

In an attempt to preserve the dimensionality of the integrals at six a number of different expansions were attempted in order to incorporate the approximate motion of these nearest neighbors. Each expansion was burdened by slow and sometimes questionable convergence. Each in turn was abandoned.

In order to see clearly the effect of allowing some approximate motion to the nearest neighbors of λ and κ it is convenient to rewrite a typical integral from equation (17) as

$$\int \phi^2(\bar{r}_\kappa - \bar{R}_\kappa)\phi^2(\bar{r}_\lambda - \bar{R}_\lambda) f^2(\bar{r}_{\lambda\kappa}) G(\bar{r}_\lambda,\bar{r}_\kappa) V_{\lambda\kappa}\, \overline{dr}_\lambda\, \overline{dr}_\kappa \tag{20}$$

where

$$G(\bar{r}_\lambda,\bar{r}_\kappa) = \prod_{s\neq\lambda,\kappa} f^2(\bar{r}_\kappa - \bar{R}_s) \prod_{\rho\neq\lambda,\kappa} f^2(\bar{r}_\lambda - \bar{R}_\rho) \tag{21}$$

Note that as shown above $G(\bar{r}_\lambda,\bar{r}_\kappa)$ expresses the correlations of molecules λ and κ to all other molecules localized at their equilibrium lattice sites. Also expressed in this manner $G(\bar{r}_\lambda,\bar{r}_\kappa) = 1.0$ corresponds to the cluster expansion result when that expansion is truncated after the two-body term. By allowing motion to the nearest neighbors to λ and κ a new $G(\bar{r}_\lambda,\bar{r}_\kappa)$ would be needed which included the effects of this motion on: (1) the correlations between the λth and κth molecules and each of their nearest neighbors; (2) the correlations between these nearest neighbors with each other; and (3) the correlations of these neighbors with all of the remaining molecules localized on their equilibrium lattice sites.

The simplest approximation is to change $G(\bar{r}_\lambda,\bar{r}_\kappa)$ to include only the effects on the correlations of the λth and κth molecules with their nearest neighbors (item 1 above). This gives

$$G(\bar{r}_\lambda,\bar{r}_\kappa) = \prod_{\substack{s\neq\lambda,\kappa \\ \neq \text{n.n. to } \kappa}} f^2(\bar{r}_\kappa - \bar{R}_s) \prod_{\substack{\rho\neq\lambda,\kappa \\ \neq \text{n.n. to } \lambda}} f^2(\bar{r}_\lambda - \bar{R}_\rho) \prod_{\substack{i=\text{n.n. to } \lambda \\ \neq \text{n.n. to } \kappa}}$$

$$\times \int \phi^2(\bar{r}_i - \bar{R}_i) f^2(\bar{r}_\lambda - \bar{r}_i)\overline{dr}_i \prod_{\substack{j=\text{n.n. to } \kappa \\ \neq \text{n.n. to } \lambda}} \int \phi^2(\bar{r}_j - \bar{R}_j)$$

$$\times f^2(\bar{r}_\kappa - \bar{r}_j)\overline{dr}_j \prod_{\substack{\ell=\text{n.n. to} \\ \lambda \text{ and } \kappa}} \int f^2(\bar{r}_\lambda - \bar{r}_\ell) f^2(\bar{r}_\kappa - \bar{r}_\ell)\phi^2(\bar{r}_\ell - \bar{R}_\ell)\overline{dr}_\ell \tag{22}$$

When molecules λ and κ do not have any nearest neighbors in common this becomes a 48-dimensional integral for a b.c.c. lattice and a 72-dimensional integral for a f.c.c. lattice. Note it is only because we have not included the effects of the motion on the correlations between these nearest neighbors themselves (item 2 above) that we can write equation (22) as the product of independent integrals.

Evaluation of $G(\bar{r}_\lambda,\bar{r}_\kappa)$ as given in equation (22) was further simplified by using the same point in three dimensional phase space for the evaluation of each of the integrals in that expression. This approximation had the effect of adding only three new dimensions to a typical integral such as the integral in equation (20) making them nine-dimensional integrals.

The remaining results are for this new formalism except where the original six-dimensional results are discussed for the sake of comparison. This new formalism gave satisfactory results over the whole range of this study. The following quantities were calculated for He^4, He^3, and H_2 for the Lennard-Jones potentials mentioned earlier. The ground-state energy as a function of density was calculated for each. At each density for which the energy was calculated the root-mean-square deviation from equilibrium was evaluated from

$$\langle r^2\rangle^{1/2} = \left\{\frac{\int \phi^2(\overline{r}_\lambda - \overline{R}_\lambda)\phi^2(\overline{r}_\kappa - \overline{R}_\kappa) f^2(\overline{r}_{\lambda\kappa}) G(\overline{r}_\lambda, \overline{r}_\kappa) |\overline{r}_\lambda - \overline{R}_\lambda|^2 \, \overline{dr}_\lambda \, \overline{dr}_\kappa}{\text{Normalization}}\right\}^{1/2} \tag{23}$$

Also at each density the single particle distribution function $R(r)$ was evaluated. $R(r)$ is given by

$$R(|\overline{r}_\lambda - \overline{R}_\lambda|) = \int \phi^2(\overline{r}_\kappa - \overline{R}_\kappa)\phi^2(\overline{r}_\lambda - \overline{R}_\lambda) f^2(\overline{r}_{\lambda\kappa}) G(\overline{r}_\lambda, \overline{r}_\kappa) \overline{dr}_\kappa \, d\Omega_\lambda \tag{24}$$

where the normalization $R(0) = 1.0$ was used. For both $\langle r^2\rangle^{1/2}$ and $R(r)$, λ and κ were nearest neighbors. From a curve fit to the energy versus density data, pressure and compressibility values were obtained. Some idea of the effect of allowing some movement of the nearest neighbors of the dynamic pair can be obtained from figure 2. Here $R(r)$ is presented for the two approximations for He^4 for two different densities. Note that the result of allowing some motion to the nearest neighbors is a spreading out of the single particle distribution function. This is just as expected and is apparently sufficient to drastically improve agreement with other ground-state properties of solid helium and hydrogen. For the sake of completeness, tabular data for the $R(r)$'s plotted in figure 2 and later figures are all presented in the last two tables of the RESULTS AND DISCUSSION section, Tables VI and VII.

B: Helium^3 Results

Results for b.c.c. He^3 are presented in Table I. In this table V is the expectation value of the energy per particle from the bare Lennard-Jones potential, $v(r_{ij})$. Also in this table T is the expectation value of the kinetic energy operator ∇_i^2 per particle. For convenience, results for He^3 and He^4 were obtained only for a b.c.c. lattice. However, He^3 at high pressures crystallizes in an f.c.c. lattice and He^4 has the h.c.p. structure for the range of densities studied here. This is not very significant since the values of the energy differ negligibly for the different lattice structures. Only the values of $\langle r^2 \rangle^{1/2}$, V, and T in the table vary with lattice structure which should be kept in mind for any comparisons with experiment or other theories.

Figure 3 contains a comparison between the results of this study, experiment, and the results of Hansen and Pollack[19] for the ground-state energy. The experimental results are from Pandorf and Edwards[24] down

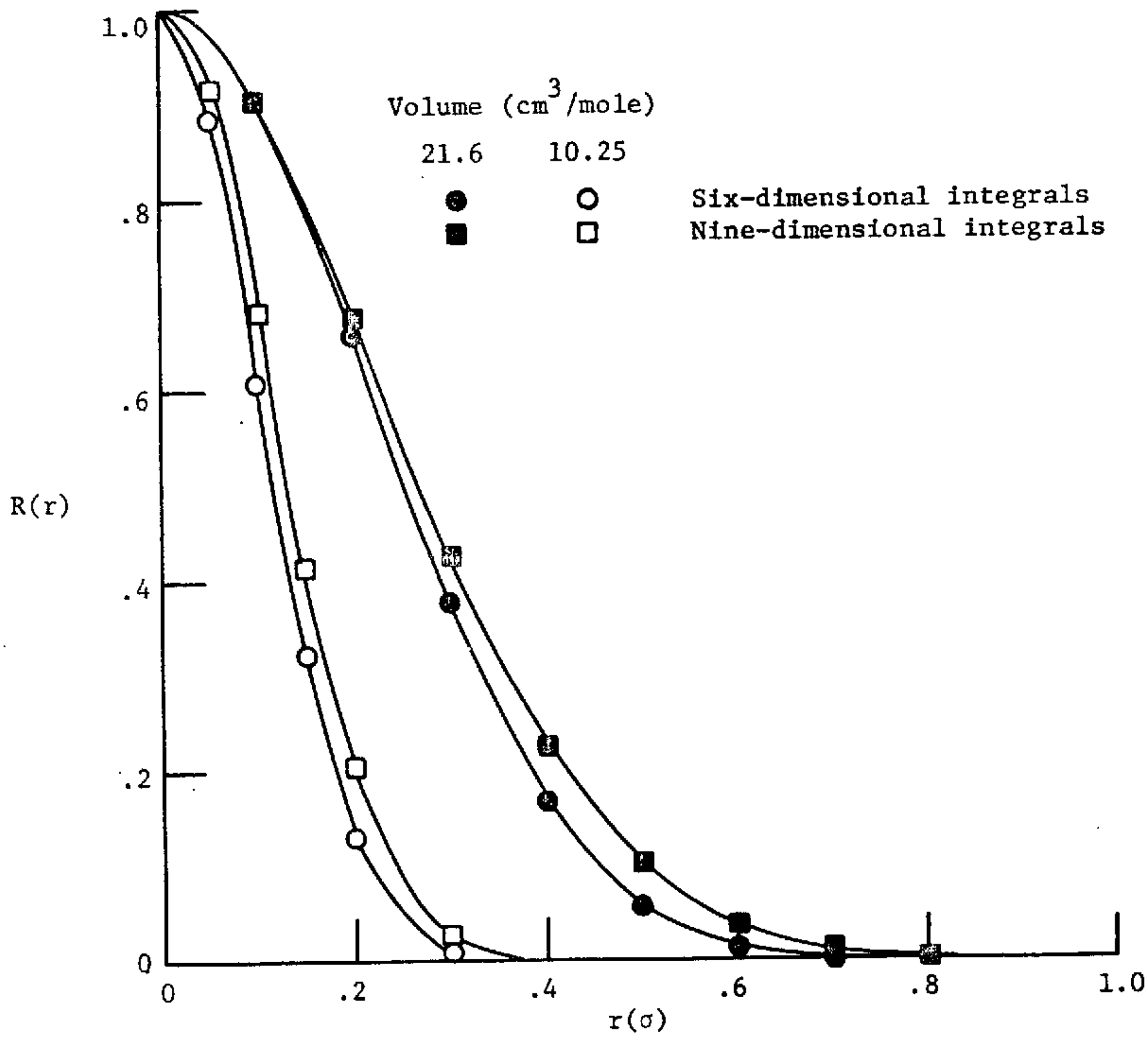

Figure 2. R(r) for two different approximations for He^4.

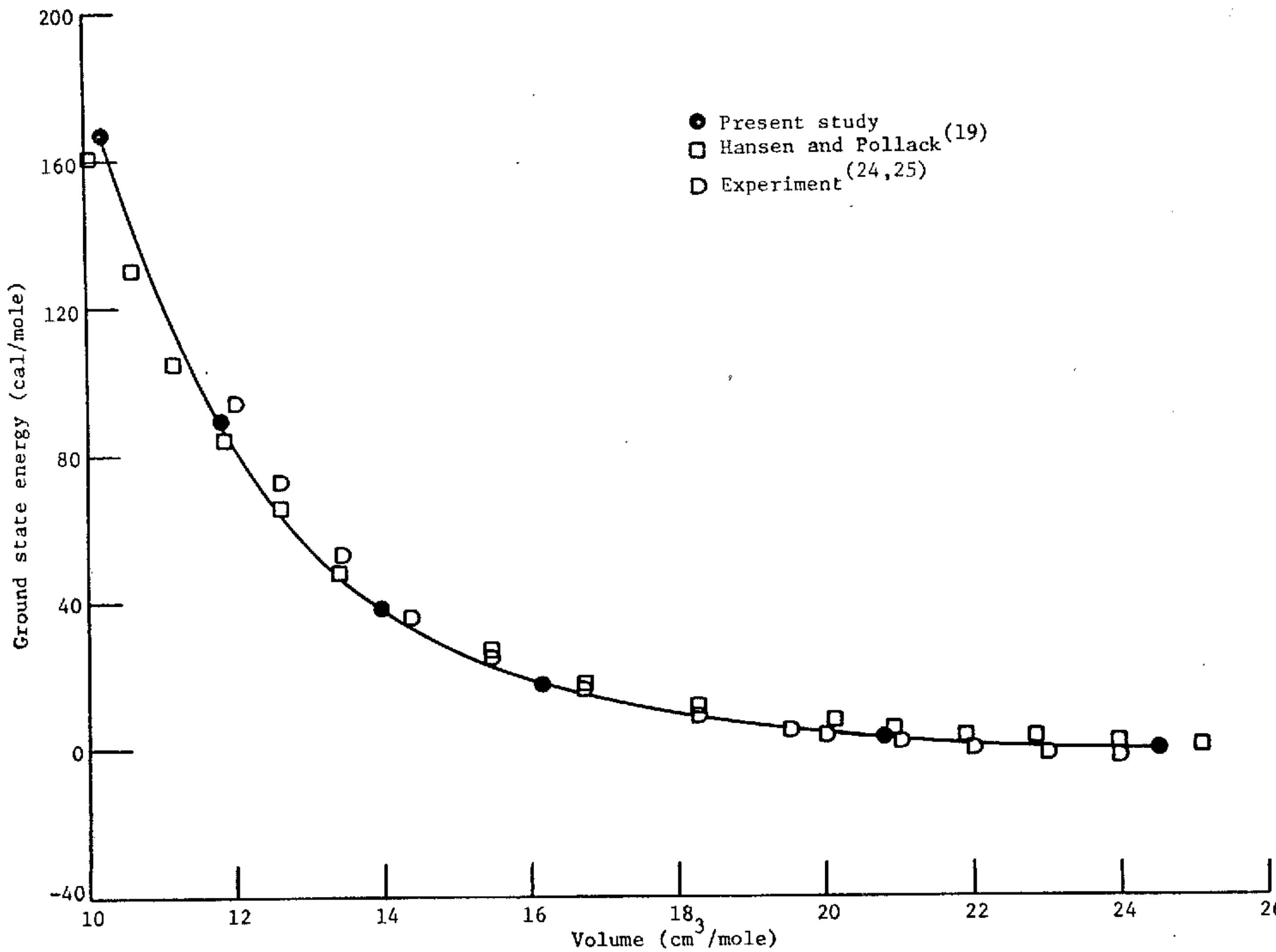

Figure 3. Ground state energy for He^3.

to a volume of 19.5 cm^3/mole. Below that, energies were computed by integrating the equation of state using pressures from Dugdale and Franck.[26] As can be seen from this figure, there is generally good agreement with experiment and with the results of Hansen and Pollack. This agreement is best at low densities (high specific volume) and the calculated energies in this range are within 2 cal/mole of the experimental values. The statistical errors for the calculated values in this range are <1 cal/mole.

At high densities the calculated values as well as the results from Hansen and Pollack[19] both begin to fall below the experimental values. This result is also the case for He^4 and is much easier to see for He^4 since experimental values exist for the entire density range studied. It was concluded in reference 19 that these discrepancies with experiment at high density are a result of inadequacies of the Lennard-Jones potential which was used, a conclusion which is shared here. As pointed out in other studies[15,19] the energy varies slowly with respect to the variational parameters in the neighborhood of the minimum. Therefore, the values for the variational parameters β and κ should not be taken as exact. Since the values of V and T taken separately vary more rapidly with β and κ these separate values have more uncertainty associated with them. It is expected that this uncertainty due to not knowing the minimizing β's and κ's exactly is less than 10 percent. In comparing the values of V and T with other studies keep in mind that these values taken separately will vary with lattice structure even though the total energy does not.

The behavior of the ground-state energy at high densities also leads to poor agreement with experimental values of pressure and compressibility in this range. Figures 4 and 5 contain comparisons of these values. The calculated values were obtained from

$$\left.\begin{aligned} P &= -\frac{\partial E_o}{\partial v} \\ \kappa &= \frac{1}{v}\frac{\partial^2 E_o}{\partial v^2} \end{aligned}\right\} \tag{25}$$

after a simple curve fit of the ground-state energy versus specific volume data. The experimental values are from references 26 and 27. Figure 6 contains plots of the single particle distribution function R(r) for different densities for He^3. Two of the related values of $\langle r^2\rangle^{1/2}$ can be compared with experimental data from reference 24. The experimental values are determined from Debye temperature data using the Debye formula[12]

$$\langle r^2\rangle = \frac{9}{4}\frac{\hbar^2}{m\kappa\theta_D} \tag{26}$$

At volumes of 24.5 cm^3/mole and 20.8 cm^3/mole the calculated values of $\langle r^2\rangle^{1/2}$ of 1.18 and 1.06 Å, respectively, are both lower than the respective experimental values of 1.38 Å and 1.15 Å.

C. Helium^4 Results

Results for b.c.c. He^4 are presented in Table II. The format of the table is identical to that of Table I. Note that the minimizing values of the variational parameters β and κ are consistently higher for He^4. A higher β more strongly localizes the individual atoms as does a higher value of κ. This is physically realistic and is due to the heavier mass of the He^4 atoms. It leads also to lower values of the root-mean-square deviation for He^4 and can be seen as a narrowing of the single particle distribution functions in figure 7.

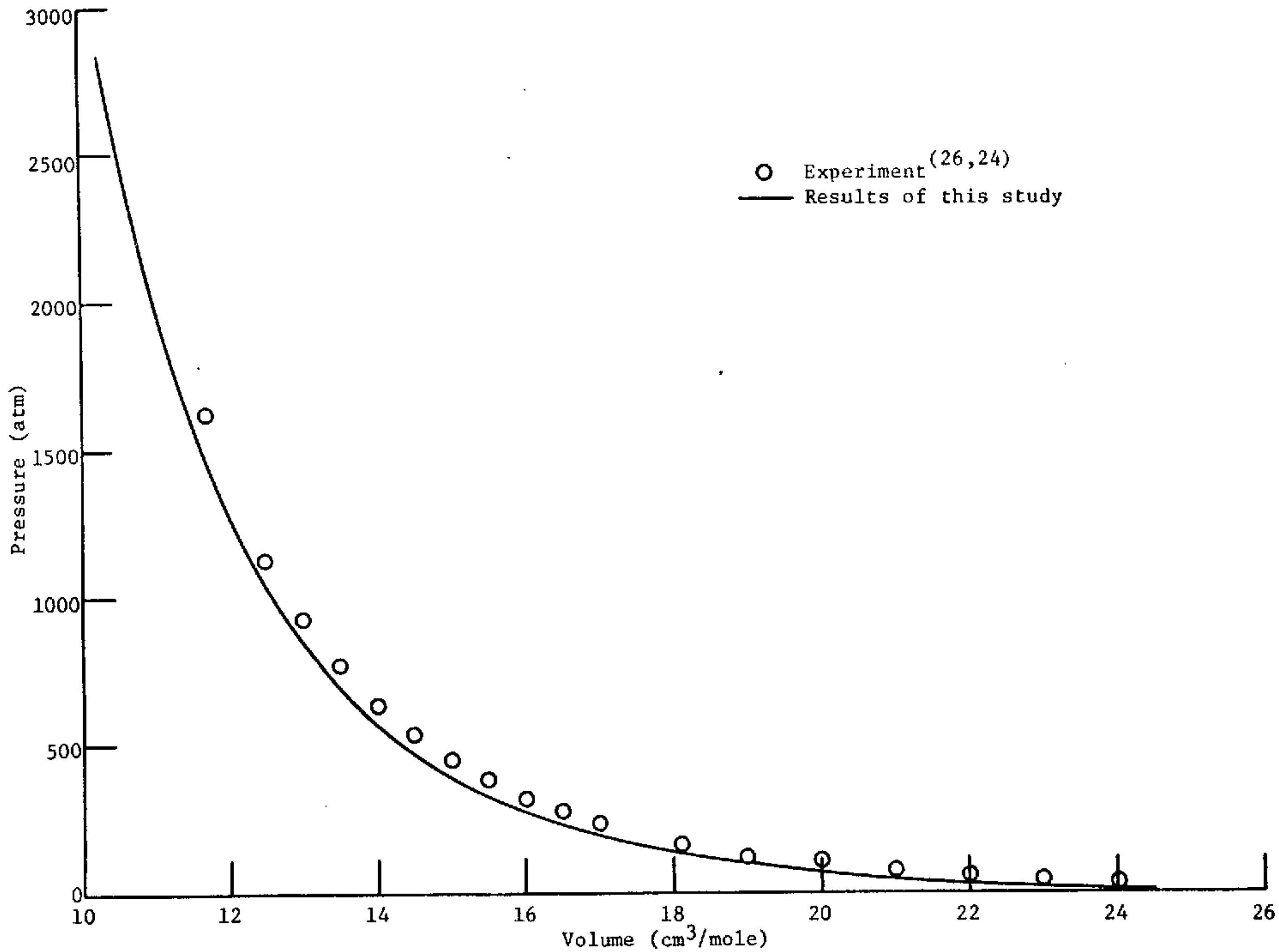

Figure 4. Pressure versus volume for He^3.

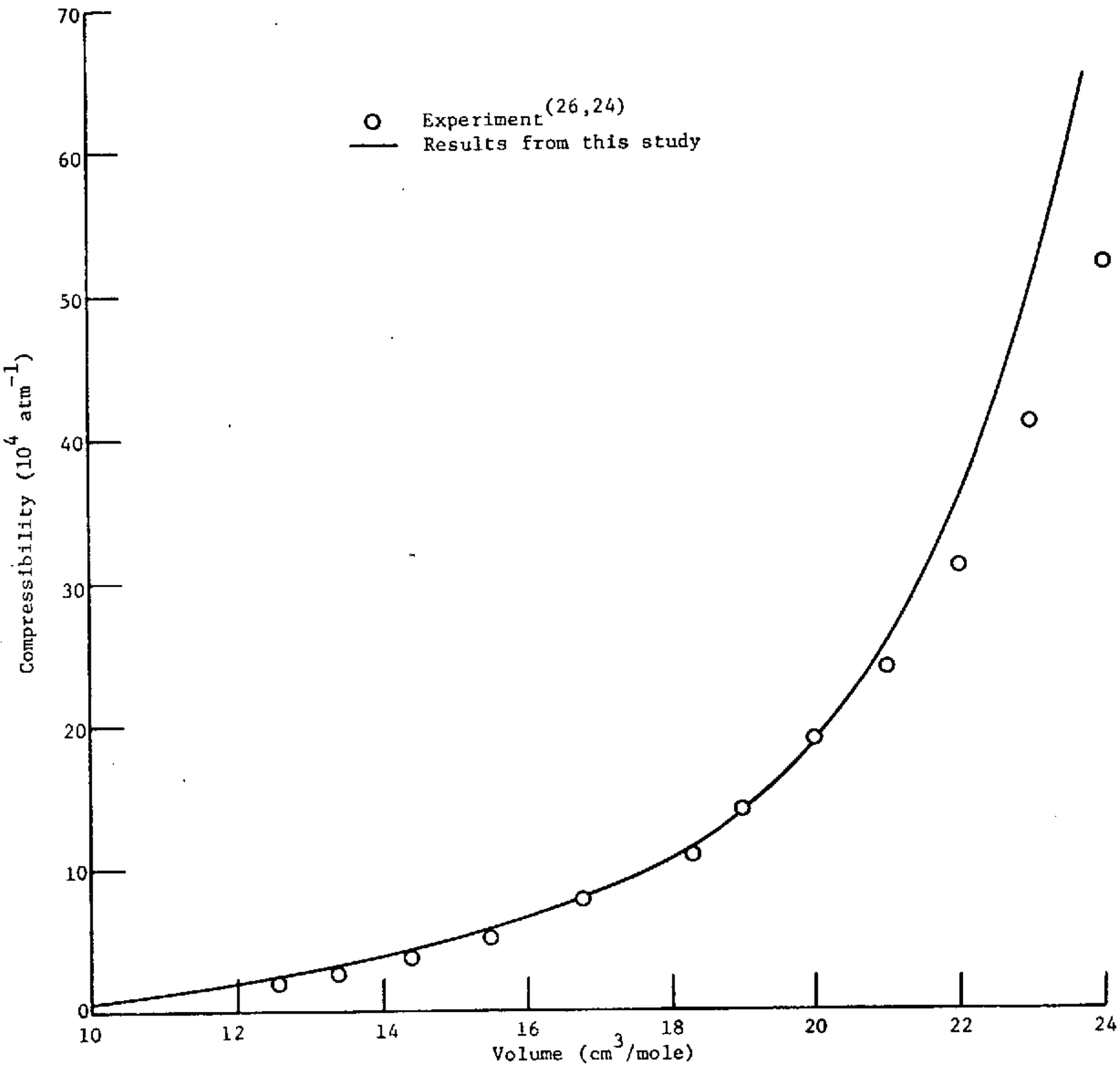

Figure 5. Compressibility versus volume for He^3.

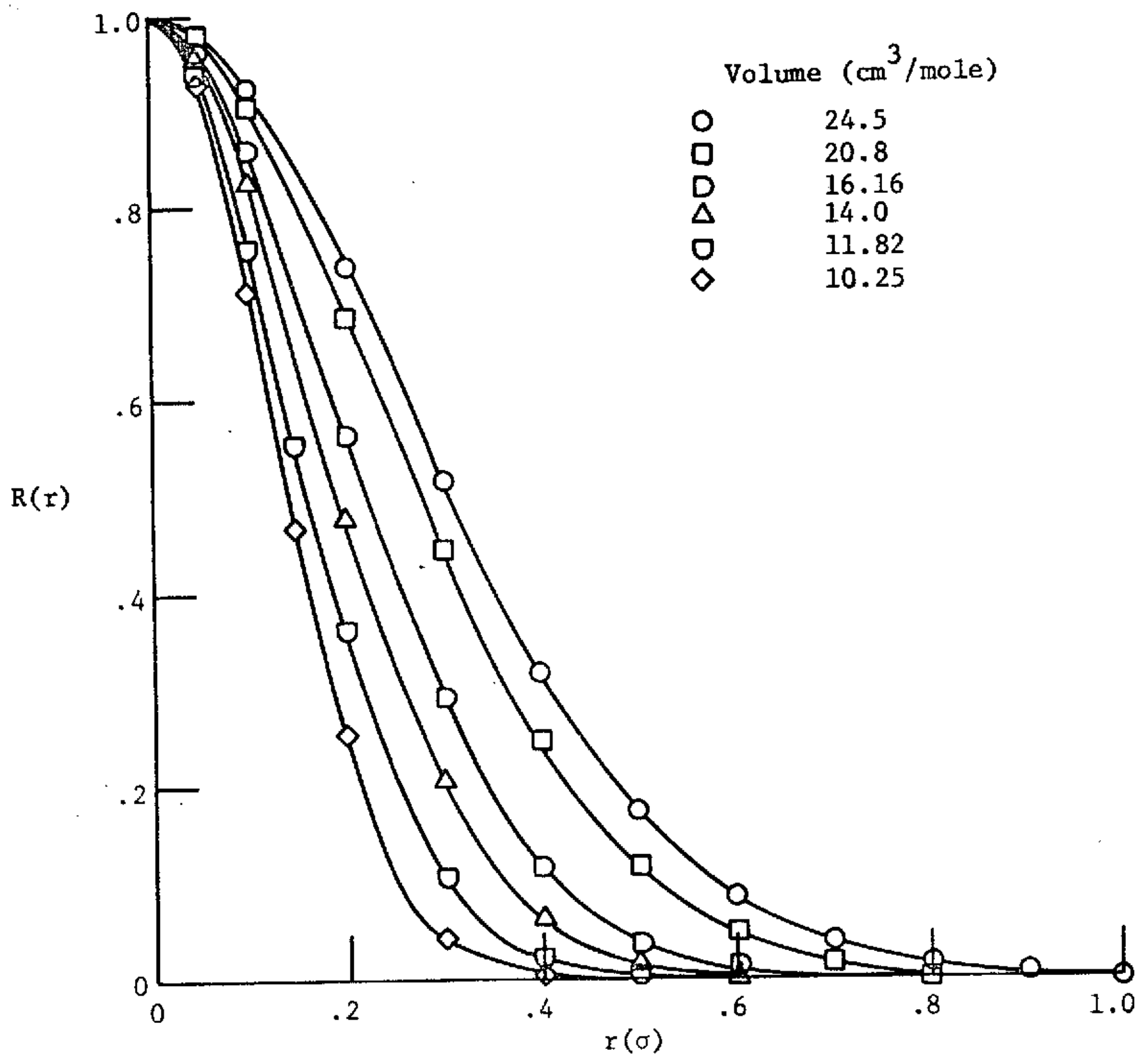

Figure 6. He^3 one particle distribution function R(r).

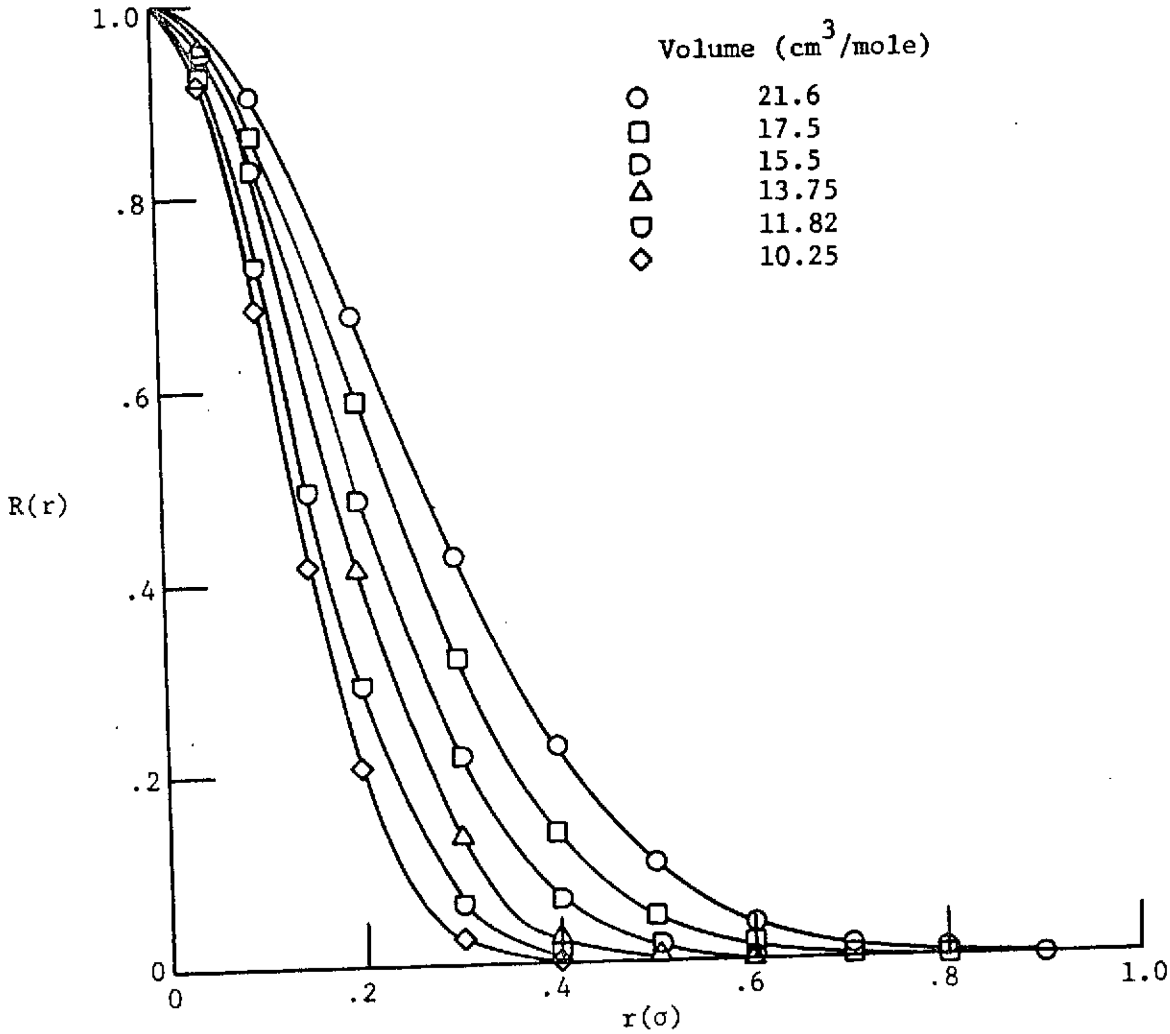

Figure 7. He^4 one particle distribution function R(r).

Figure 8 contains a comparison of the single particle distribution function and $e^{-\beta r^2}$ for He^4 at two specific volumes. The latter, i.e., $e^{-\beta r^2}$, would be the single particle distribution function if the wave function did not contain two-body correlation functions. This figure gives some indication then of how much of the localizing of individual molecules on lattice sites is due to the effect of the two-body correlation functions. Note that at the lower specific volume the two-body correlation functions still are responsible for some of the localizing. This supports Hansen and Pollack's[19] contention that these correlations are still important at high pressures. In addition, this figure contains a comparison with Hansen and Levesque's[15] R(r) for He^4 at a volume of 21.5 cm^3/mole. The two R(r)'s appear to be very similar.

Figure 9 contains a comparison between the results of this study, experiment, and the results of Hansen and Pollack[19] for the ground-state energy of He^4. The experimental data are from references 23 and 26. Below 11.5 cm^3/mole the experimental energies are obtained by integrating the experimental equation of state. As for He^3 there is good agreement with experiment except at the higher densities (low specific volume). As pointed out earlier this is attributed to inadequacies in the Lennard-Jones potential which was used. An interesting feature of figure 3 and figure 9 is that the theoretical values from this study and reference 19 both are above the experimental values at low densities and are below the experimental values at high densities. In each region for both He^3 and He^4 the results of this study agree more closely with the experimental values. It is not completely clear why this is the case. It is possible that the use of another lattice structure at the high densities would yield a slightly lower ground

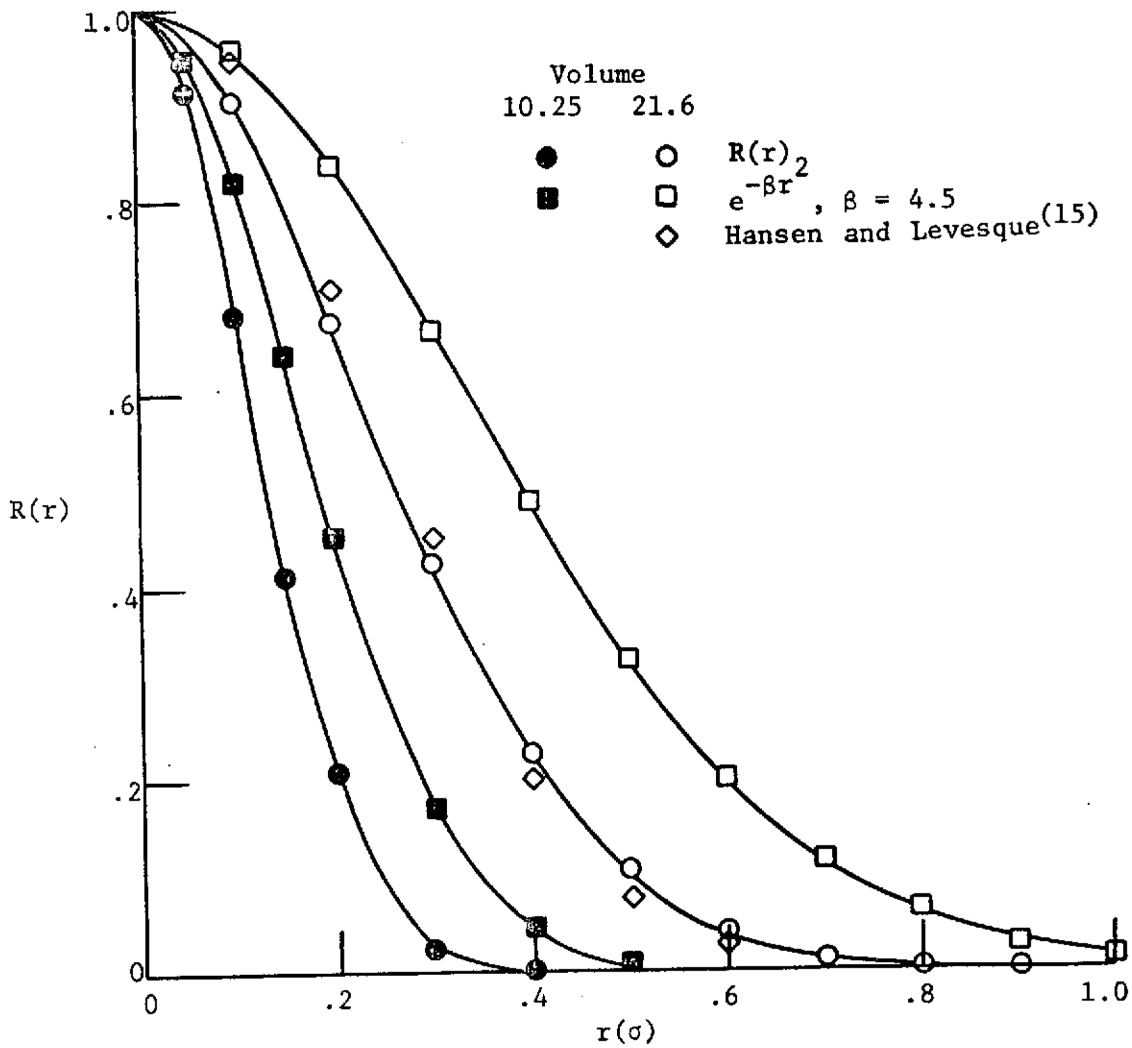

Figure 8. Comparison of $R(r)$ and $e^{-\beta r^2}$ for He^4 at two different volumes.

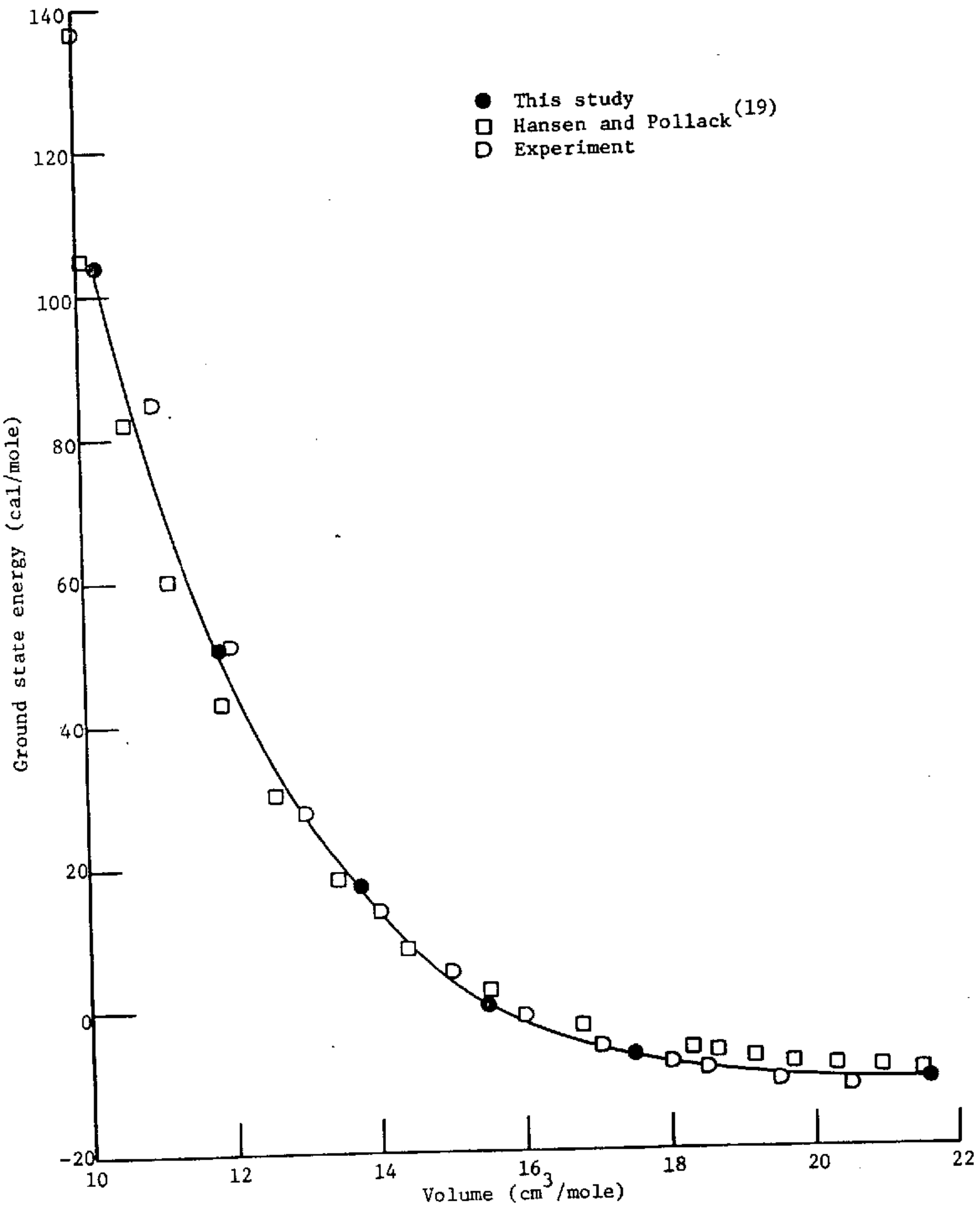

Figure 9. Ground state energy for He^4.

state energy. This would then lead to closer agreement with the Monte Carlo results in the high density region; however, the agreement even in this region is remarkably good.

The differences in the shape of the energy versus density curve lead to correspondingly poor agreement with experimental values of pressure and compressibility. These results are presented in figures 10 and 11 along with experimental values from references 23 and 26. As with He^3, the theoretical values are lower than experimental values over the entire range of densities with the worst agreement at the high densities.

The values for the root-mean-square deviation are not compared with experimental estimates from Debye temperature data since the calculated values are for a b.c.c. lattice and the experimental values would be from a hexagonal close-packed lattice.

It should be pointed out that even though the Monte Carlo calculations of Hansen and coworkers should be fairly exact, there still exist differences in the computed ground state energies from Hansen and Pollack[19] and Hansen and Levesque.[15] These differences amount to as much as 2 cal/mole even though the statistical errors quoted are 1 cal/mole and 0.4 cal/mole, respectively.

D. Hydrogen Results

There exists even more uncertainty in the interatomic potential for molecular hydrogen than for the corresponding potential for helium. Because of this, the calculations for hydrogen are less extensive than for helium. As for helium there exist for hydrogen Monte Carlo calculations[28] as well as experimental data[29] with which to compare the results of this study. The wave function chosen is the same as the one

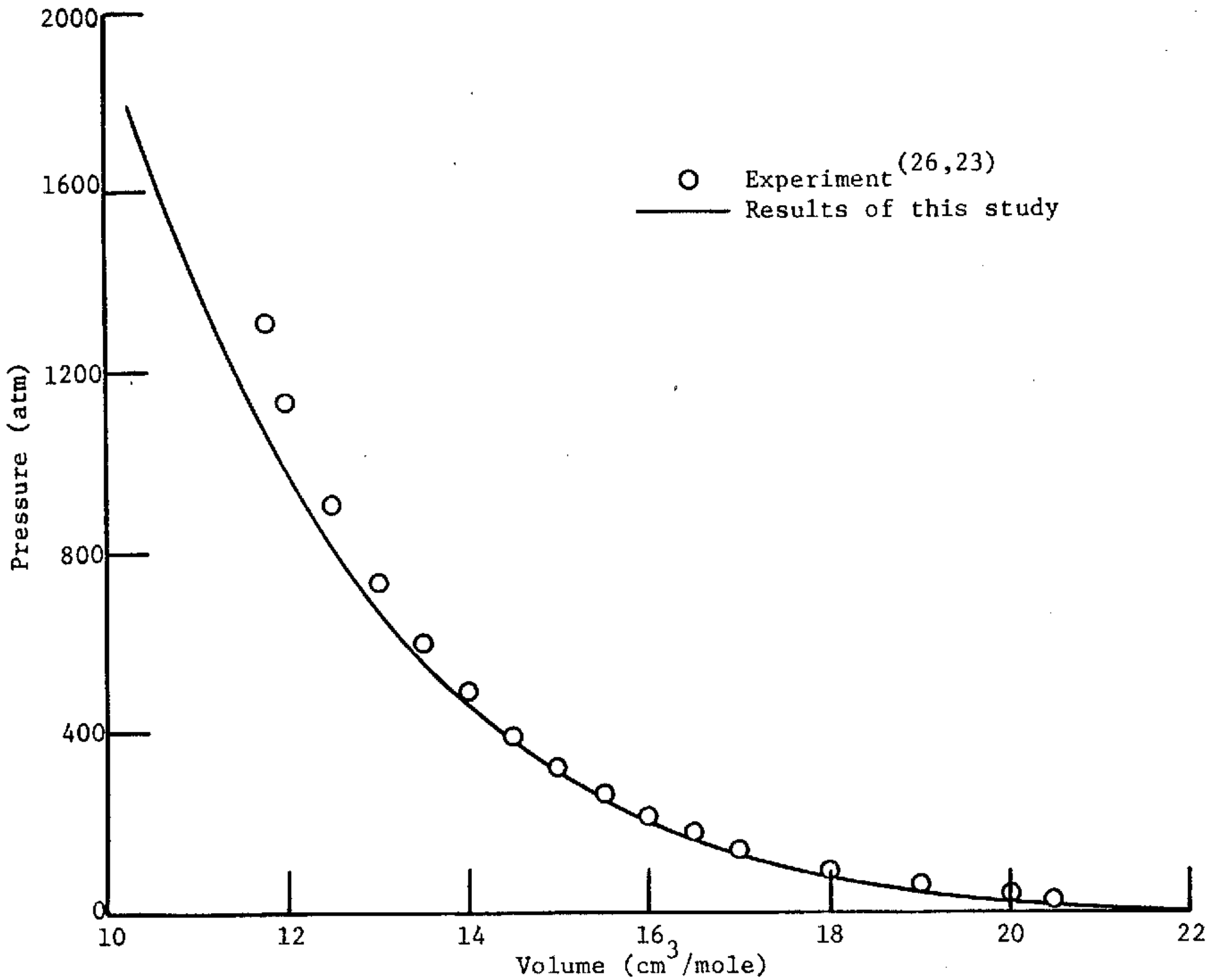

Figure 10. Pressure versus volume for He^4.

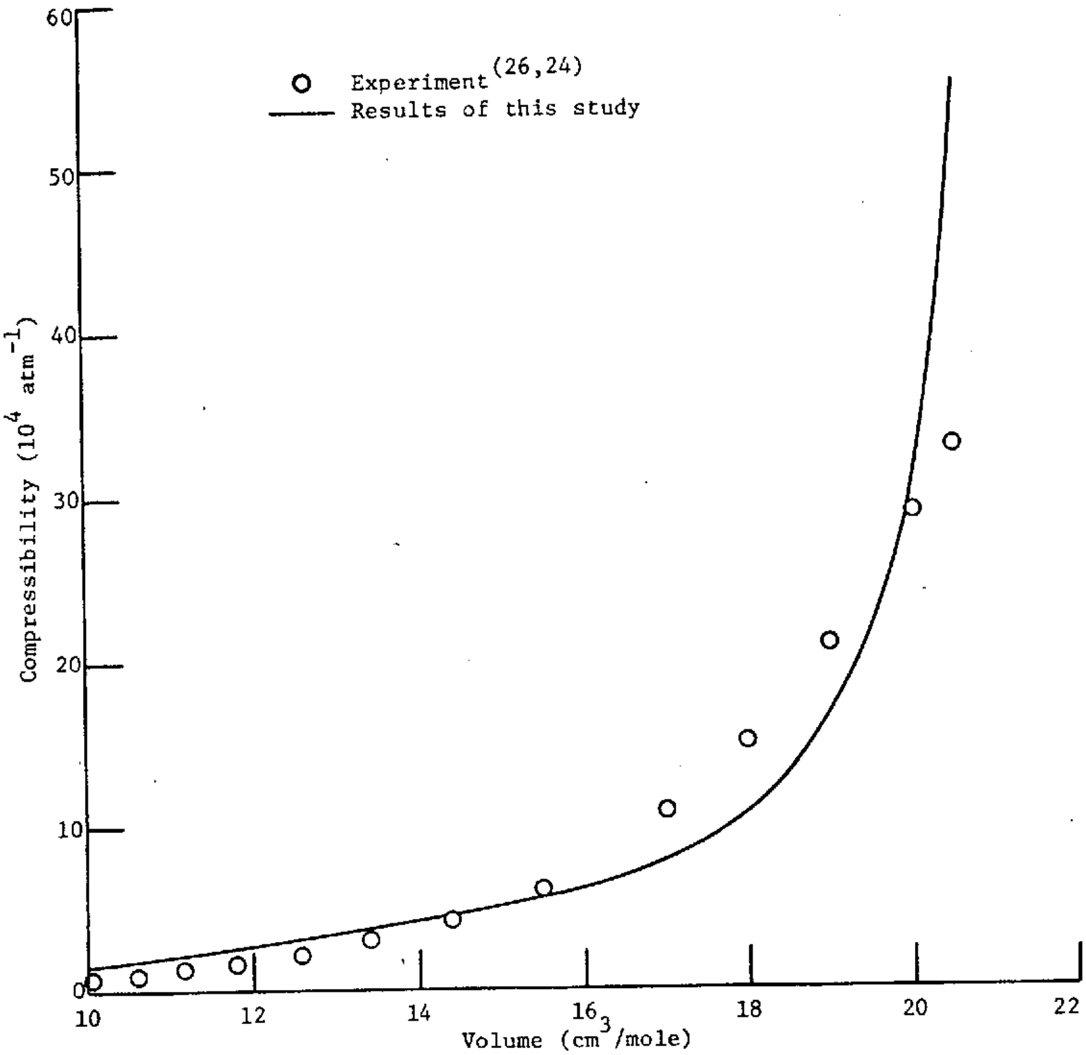

Figure 11. Compressibility versus volume for He^4.

used for the helium studies. The use of a spherically symmetric two-body correlation function $f(r)$ which is independent of the orientation of the H_2 molecules requires some justification. Ordinarily one would picture the H_2 molecules as something resembling a dumbbell. However, calculations by Kolos and Roothan[30] have shown that the deviation from sphericity for the H_2 molecule is only ≈8 percent. Their calculations lead to $\langle r^2\rangle^{1/2} \approx 0.84$ Å and $\langle 3Z^2\rangle^{1/2} \approx 0.92$ Å. For a spherical molecule $\langle r^2\rangle = \langle X^2 + Y^2 + Z^2\rangle = \langle 3Z^2\rangle$. Therefore, the use of a spherically symmetric two-body correlation function and interatomic potential are not as bad as one would at first imagine.

The results of this study using a Lennard-Jones 6-12 potential are presented in Table III. The ground-state energy at a volume of 22.65 cm^3/mole is -170 cal/mole. This is the same value obtained by Bruce[28] for a volume of 23.08 cm^3/mole and is slightly higher than Stewart's[29] experimental value of -186 cal/mole at a volume of 22.65 cm^3/mole.

The ground-state energies as a function of volume are compared with Bruce's values in figure 12. The results of this study start to drop below Bruce's values at around a volume of 15 cm^3/mole and differ by over 100 cal/mole at the lowest volumes studied here. The statistical errors in this region are <10 cal/mole. Most of this difference is due to the different parameters used in the Lennard-Jones potential in this study. As pointed out previously, these values were $\varepsilon = 37^\circ$ K and $\sigma = 2.93$ Å. This compares to the values used by Bruce of $\varepsilon = 36.7^\circ$ K and $\sigma = 2.958$ Å. At these high densities differences in the interatomic potential can easily lead to differences of a couple of hundred calories per mole in the ground-state energy. To show this

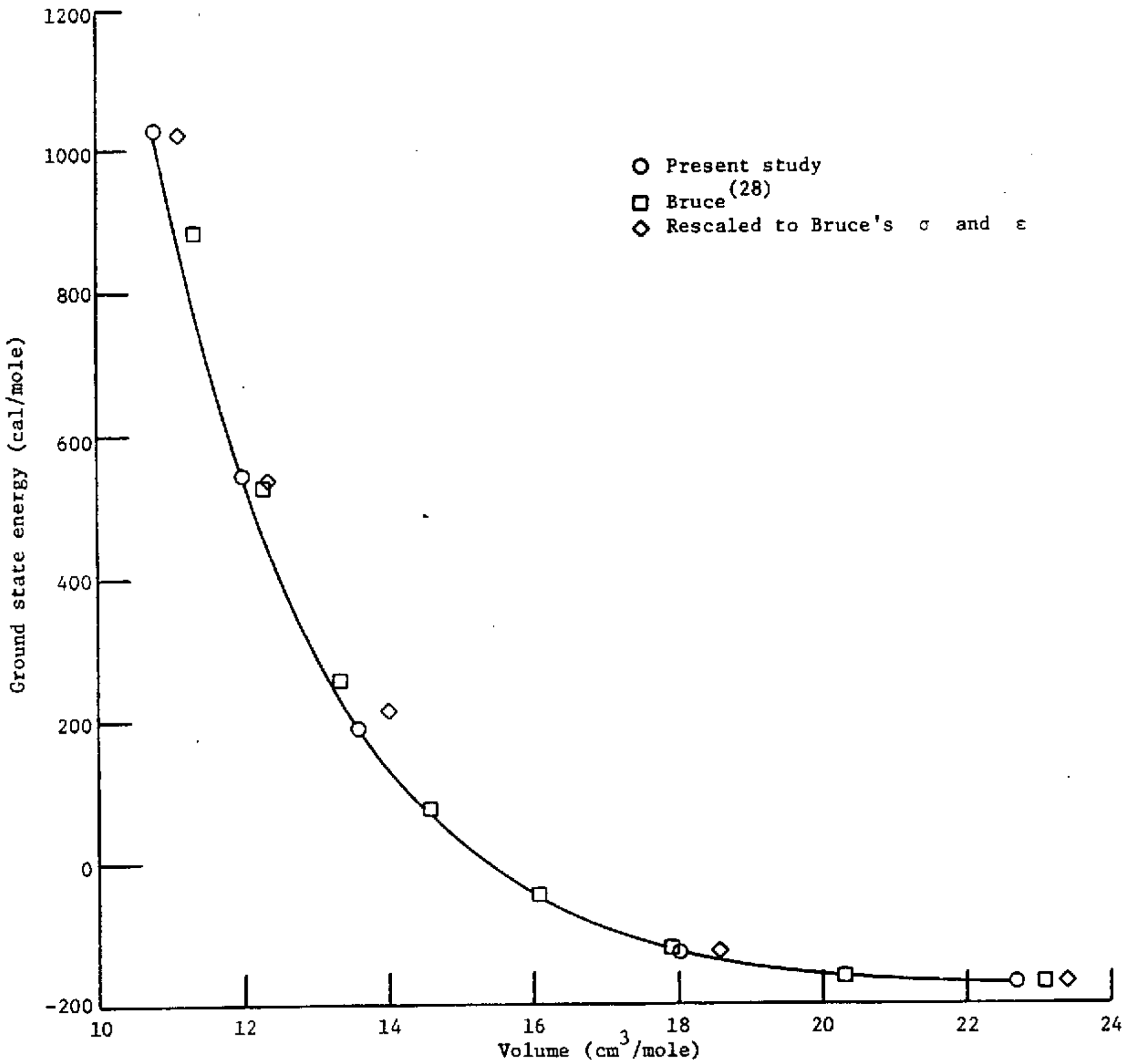

Figure 12. Ground state energy for H_2.

effect the results from this study have been rescaled to Bruce's values of σ and ε and are also presented in figure 12. The agreement is now excellent at the high densities but not as good in the intermediate range.

Another indication of the amount of uncertainty possible in the energies calculated using the Monte Carlo methods of Hansen and co-workers is Bruce's statement that two different initial particle configurations led to energies that varied by as much as 4 to 6 cal/mole. This is in addition to any statistical errors in his results.

The pressure versus volume results for this study are compared with Bruce's Monte Carlo results and with Stewart's experimental data in figure 13. The pressure data falls below Bruce's values at low volumes, a direct consequence of the lower energies in this region. This brings the pressures from this study closer to Stewart's experimental data. This is due to the differences in interatomic potential previously pointed out. The resulting pressures are still much higher than Stewart's values, a result consistent with all of the theoretical studies done to date. Again rescaled values using Bruce's values of σ and ε agree very well with his values for the pressure. Most of the studies now in progress on hydrogen are aimed at determining an interatomic potential which yields theoretical results that fit more closely Stewart's pressure data.

E. Effects of Approximations

The biggest approximation is, of course, the molecular field approximation itself. The effect of studying the dynamic motion of pairs of molecules in a lattice where most of the remaining molecules are fixed on their equilibrium lattice sites can only be determined

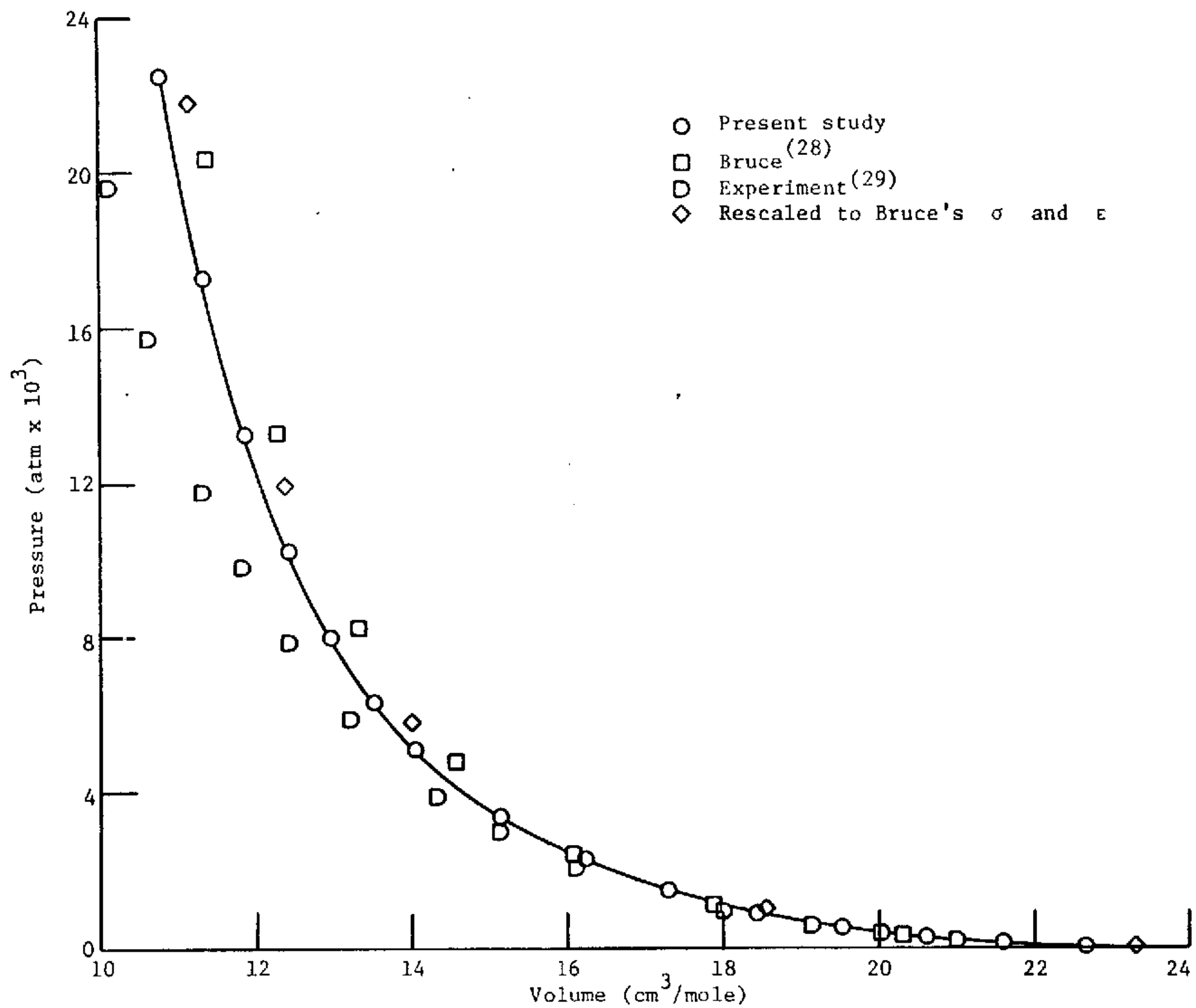

Figure 13. Pressure versus volume for H_2.

from the comparisons with experiment. This approach in general seems to be reasonable based on the agreement with experiment.

The inclusion of approximate motion of the nearest neighbors to the dynamic pair λ and κ had a dramatic effect on the results. It is important therefore to reiterate what this approximation includes and what it does not include. This approximation treats exactly the correlation of both λ and κ to each of their nearest neighbors. It does not treat exactly the correlation of these nearest neighbors with each other or with the remaining molecules in the lattice. This would have an indirect effect on the molecules λ and κ. This effect is apparently quite small as indicated by the close agreement with experiment with the present formalism. The use of only three new variables to evaluate the effects of motion of the nearest neighbors of λ and κ worked quite well again as indicated by the results.

As pointed out previously, other approximations have been made in the evaluation of equation (17). First the integrals were calculated exactly only for the first ten nearest neighbor shells. The contributions from the remaining shells are evaluated for a static lattice. It was found that over the range of densities studied, the energy could be determined to within ~1 cal/mole if only the contributions from the first four nearest neighbor shells were calculated exactly, which is the approximation used in the "exact" Monte Carlo studies. Evaluating contributions from only ten shells exactly leads to a negligible error. The static lattice sum is cut off after thirty-eight nearest neighbor shells. This again gives negligible error. Some idea of the magnitudes of the contributions from different nearest neighbor shells can be seen in Table IV. This table contains contributions from different groups of nearest neighbor shells for both T and V for He^4 at 21.6 cm^3/mole, and 10.25 cm^3/mole. As can be seen from this table, the contributions from the first two nearest neighbor shells are very large at the low density. The contributions from the other shells become increasingly important with higher densities; however, the contributions from the first four or five shells dominate the total energy even at these higher densities.

Another important approximation is the cutoff of the product of two-body correlation functions. These products contained the exact correlations of the λth and κth molecules to only their first, second, and third nearest neighbors. The values of the correlation function outside this range were unity. Some idea of the effect of this approximation can be seen in Table V where $\langle T \rangle$, $\langle V \rangle$, and E_o are presented for a typical He^4 calculation at 21.6 cm^3/mole as a function of the nearest neighbor shells contained exactly in this product. As can be seen in this table, these results converge quickly even though the f(r) used in this study is a fairly long-ranged two-body correlation function. Most of the results for H_2 were obtained with a second nearest neighbor cutoff in these products to save computation time. Again this approximation results in negligible errors.

The statistical errors ranged from less than 1 cal/mole at the low densities to as much as 3 to 4 cal/mole at 10.25 cm^3/mole for the helium ground-state energies. The statistical errors for hydrogen were a factor of two to three higher. Because of the uncertainties in the interaction potential for hydrogen it was not felt warranted to spend more computation time on these results.

It is felt that the cumulative effect of errors introduced by the above approximations is indeed small and would not effect any of the conclusions made from comparisons with experimental data.

Since most of the results have been compared with Monte Carlo results, a discussion of some of the limitations of that approach might be useful. These Monte Carlo calculations represented the best agreement with experiment to date. However, as pointed out earlier, calculations by Hansen and Pollack[19] and Hansen and Levesque[15] for helium differ by as much as 2 cal/mole even though the statistical errors quoted are 1 cal/mole and 0.4 cal/mole, respectively. Also, as pointed out previously, Bruce[28] obtained results which differed by as much as 6 cal/mole depending on the starting configuration used. This was in addition to any statistical error.

The Monte Carlo method is naturally limited to a finite volume of molecules that can be treated exactly. This is usually less than 1000 particles enclosed in a box with periodic boundary conditions. This and other approximations, such as letting each particle interact exactly with only four or five nearest neighbor shells, add possible errors to the Monte Carlo results.

In addition, W. W. Wood[31] points out the likelihood that at high densities it is quite possible that the Monte Carlo techniques used may not properly sample phase space. This might effect substantially the results at these densities.

IV. CONCLUDING REMARKS

The molecular field approximation as first formulated (six-dimensional integrals) led to undesirable results. The new formulation which allows in an approximate fashion the motion of nearest neighbors of the dynamic pair gives much better results. None of the many approximate theories of quantum crystals proposed to date agree as well with experimental data and the Monte Carlo results as do the results of this study. In addition, limitations on the two-body correlation functions necessary for the various cluster expansion approaches are not imposed by the molecular field approximation.

The molecular field approximation is, therefore, a valuable tool for the study of properties of quantum crystals. The results of this study can easily be extended to include different trial wave functions, different potentials, and also much higher densities for a thorough investigation of the properties of quantum crystals. There are some indications that random walk Monte Carlo methods may have difficulty in properly sampling phase space at very high densities. The molecular field approximation might therefore be quite useful at these densities.

REFERENCES

1. Jastrow, R. Physical Review 98, 1479 (1955).
2. Nosanow, L. H. Physical Review 146, 120 (1966).
3. Mullin, W. J., and Nosanow, L. H. Physical Review Letters 14, 133 (1965).
4. Hetherington, J. H., Mullin, W. J., and Nosanow, L. H. Physical Review 154, 175 (1967).
5. Brueckner, K. A., and Frohberg, J. Progress in Theoretical Physics (Kyoto), Supplement 383 (1965).
6. Massey, W. E., and Woo, C. W. Physical Review 169, 241 (1968).
7. Brueckner, K. A., and Thieberger, R. Physical Review 178, 362 (1969).
8. Koehler, T. R. Physical Review 18, 654 (1967).
9. Koehler, T. R. Physical Review 165, 942 (1968).
10. Gillis, N. S., Koehler, T. R., and Werthamer, N. R. Physical Review 175, 1110 (1968).
11. Guyer, R. A. Solid State Communications 7, 315 (1969).
12. Guyer, R. A. Solid State Physics 23, 413 (1969).
13. Werthamer, N. R. American Journal of Physics 37, No. 8, 763 (1969).
14. Horner, H. Physical Review 1, 1712 (1970).
15. Hansen, J. P., and Levesque, D. Physical Review 165, 293 (1968).
16. Hansen, J. P. Physics Letters 30A, 214 (1969).
17. Hansen, J. P. Physics Letters 34A, 25 (1971).
18. Hansen, J. P. Physical Review A2, 221 (1970).
19. Hansen, J. P. and Pollack, E. L. Physical Review A5, 2651 (1972).
20. Jackson, H. W., and Feenberg, E. Annals of Physics 15, 266 (1961).

21. Etters, R. D., Raich, J. C., and Danilowicz, R. L. Lettere al Nuovo Cimento, Serie I., Vol. 4, pp. 667-674.

22. Hammersley, J. M. and Handscomb, D. C., Monte Carlo Methods, John Wiley & Sons, Inc., New York, N.Y., 1964.

23. Edwards, D. O. and Pandorf, R. C. Physical Review 140, A816 (1965).

24. Pandorf, R. C., and Edwards, D. O. Physical Review 169, 222 (1968).

25. McMahan, A. K. Journal of Low Temperature Physics, Vol. 18, Nos. 1/2, 1972.

26. Dugdale, J. S. and Franck, J. P. Philosophical Transactions of the Royal Society 257, 1 (1964).

27. Straty, G. C. and Adams, E. D. Physical Review 169, 232 (1968).

28. Bruce, T. A. Physical Review B5, 4170 (1972).

29. Stewart, J. W. Journal of Physics and Chemistry of Solids 1, 146 (1956).

30. Kolos, W. and Roothaan, C. C. J. Review of Modern Physics 32, 219 (1960).

31. Wood, W. W. Physics of Simple Liquids, North-Holland Publ. Co., Amsterdam, 1968.

TABLE I. - b.c.c. He^3 RESULTS

Volume (cm^3/mole)	$\langle V \rangle$ (cal/mole)	$\langle T \rangle$ (cal/mole)	E_0 (cal/mole)	Pressure (atm)	Compressibility (10^4 atm^{-1})	$\langle r^2 \rangle^{1/2}$ (Å)	β (σ^{-2})	κ (σ^{-1})
24.50	-44.1	43.6	-0.5			1.18	3.5	1.11
20.80	-53.6	56.4	2.8	50	23.8	1.06	4.1	1.11
16.16	-64.2	81.7	17.5	260	7.0	.85	6.5	1.08
14.00	-64.0	102.2	38.2	565	3.9	.75	8.7	1.06
11.82	-49.2	138.5	89.3	1380	1.8	.62	12.5	1.04
10.25	-16.5	183.3	166.8	2820	.7	.52	19.0	1.02

TABLE II. - b.c.c. He^4 RESULTS

Volume (cm^3/mole)	$\langle V \rangle$ (cal/mole)	$\langle T \rangle$ (cal/mole)	E_0 (cal/mole)	Pressure (atm)	Compressibility (10^4 atm^{-1})	$\langle r^2 \rangle^{1/2}$ (Å)	β (σ^{-2})	κ (σ^{-1})
21.60	-54.6	44.3	-10.3			1.03	4.5	1.13
17.50	-68.1	61.3	-6.8	93	9.0	.83	5.7	1.13
15.5	-77.3	77.5	.2	250	6.0	.76	8.0	1.12
13.75	-80.4	97.5	17.1	500	4.0	.64	11.5	1.11
11.82	-80.4	130.8	50.4	1035	2.6	.56	15.0	1.10
10.25	-62.1	165.9	103.8	1790	1.6	.48	20.0	1.10

TABLE III. - f.c.c. H_2 RESULTS

Volume (cm^3/mole)	V (cal/mole)	T (cal/mole)	E_o (cal/mole)	Pressure (atm)	β (σ^{-2})	κ (σ^{-1})
22.65	-301	131	-170		6	1.19
18.00	-376	252	-124	1 100	30	1.14
13.60	-298	487	189	6 350	67	1.12
12.00	-51	595	544	12 400	80	1.11
10.80	318	707	1025	22 500	95	1.10

TABLE IV. - CONTRIBUTIONS FROM DIFFERENT NEAREST NEIGHBOR SHELLS

Volume (cm^3/mole)	Nearest neighbor shell	Contribution to V (cal/mole)		Contribution to T (cal/mole)		Contribution to H (cal/mole)	
		Exact	Rigid lattice	Exact	Rigid lattice	Exact	Rigid lattice
21.60	1st	-29.90		25.00		-4.90	
	2nd	-13.27		4.75		-8.52	
	3rd-10th	-10.66		1.94		-8.72	
	11th-38th	≈-0.77	-0.77	≈.06	0.06	≈-.71	-0.71
				$\frac{3\hbar^2\beta}{4m}$=12.51		+12.51	
	Total	-54.60		44.26		-10.34	
10.25	1st	+17.53		84.90		+102.43	
	2nd	-38.90		17.94		-20.96	
	3rd	-16.37		3.68		-12.69	
	4th	-11.03	-11.38	2.05	1.99	-8.98	-9.39
	5th-10th	-9.85	-9.92	1.40	1.40	-8.45	-8.52
	11th-38th	≈-3.47	-3.47	≈.29	.29	-3.18	-3.18
				$\frac{3\hbar^2\beta}{4m}$=55.60		+55.60	
	Total	-62.09		165.86		103.77	

TABLE V. - PRODUCT OF CORRELATION FUNCTIONS APPROXIMATION

V (cal/mole)	T (cal/mole)	H (cal/mole)	Exact product of f(r)'s cutoff after
-48.20	40.80	-7.46	1st nearest neighbors
-50.35	39.90	-10.45	2nd nearest neighbors
-50.20	39.90	-10.30	3rd nearest neighbors

TABLE VI. - R(r) DATA FOR He^3

Volume	r(σ)										
(cm^3/mole)	0	0.05	0.10	0.15	0.20	0.30	0.40	0.50	0.60	0.70	0.80
10.25	1.00	0.928	0.717	0.466	0.254	0.042	0.0035				
11.82	1.00	.935	.757	.559	.363	.107	.019	0.0018			
14.00	1.00	.957	.824		.480	.206	.060	.012	0.0015		
16.16	1.00	.961	.859		.567	.293	.117	.036	.0078		
20.8	1.00	.975	.905		.688	.445	.246	.116	.046	0.0148	0.0039
24.5	1.00		.922		.738	.515	.317	.173	.083	.034	.012

TABLE VII. - R(r) DATA FOR He^4

Volume (cm^3/mole)	r(σ)										
	0.0	0.05	0.10	0.15	0.20	0.30	0.40	0.50	0.60	0.70	0.80
10.25	1.00	0.916	0.681	0.417	0.207	0.027	0.0012				
11.82	1.00	.922	.730	.495	.292	.064	.0070				
13.75	1.00	.955	.809		.412	.133	.026	.0028			
15.50	1.00		.829		.484	.217	.068	.019	.0022		
17.50	1.00		.862		.587	.319	.137	.045	.011	.0019	
21.60	1.00		.901		.675	.424	.227	.102	.038	.011	.0028
Six-Dimensional Formalism											
10.25	1.00	0.885	0.610	0.323	0.130	0.0084	0.00015				
21.60	1.00	.975	.902		.657	.380	.168	0.054	0.013	0.0022	0.00032

APPENDIX A

SYMBOLS

E	energy
$f(r)$	two-body correlation function
G	defined by eqs. (21) and (22)
H	Hamiltonian
$\hbar$	Planck's constant divided by 2π
$\hat{i}$	unit vector in x direction
J	exchange integral
$\hat{j}$	unit vector in y direction
m	mass
N	number of molecules in the crystal lattice
p	pressure
$\overline{R}_i$	vector to equilibrium position of the i^{th} molecule
$\overline{R}_{ij}$	$= \overline{R}_i - \overline{R}_j$, vector joining the equilibrium positions of the i^{th} and j^{th} molecules
$R(r)$	single particle distribution function defined by eq. (24)
r	distance (depending on usage $\overline{r} = \lvert\overline{r}_i - \overline{r}_j\rvert$ or $r = \lvert\overline{r}_i - \overline{R}_i\rvert$, etc.)
r	$= \lvert\overline{r}_\kappa - \overline{R}_\kappa\rvert$, distance that κ^{th} molecule is from its equilibrium position
$\langle r^2\rangle^{1/2}$	root mean square deviation from equilibrium defined by eq. (23)
$\overline{r}_i$	vector to position of i^{th} molecule
$\overline{dr}_i$	volume element for the i^{th} molecule
$\overline{r}_{ij}$	$= \overline{r}_i - \overline{r}_j$, vector joining the i^{th} and j^{th} molecules

T	kinetic energy per molecule
V	potential energy per molecule
V_{ij}	defined by eq. (12)
v	specific volume (appears only in eq. (25))
x	cartesian coordinate
y	cartesian coordinate
y	$= \lvert\bar{r}_s - \bar{R}_s\rvert$ and $= \lvert\bar{r}_\rho - \bar{R}_\rho\rvert$, distance that the nearest neighbors to the λth and κth molecules are from their equilibrium positions
z	cartesian coordinate
z	$= \lvert\bar{r}_\lambda - \bar{R}_\lambda\rvert$, distance that the λth molecule is from its equilibrium position
β	variational parameter in $\phi(r)$
δ	Dirac δ function
$\bar{\nabla}$	gradient
∇^2	Laplacian
ε	depth of potential well
θ	spherical coordinate
θ_D	Debye temperature
$\hat{\kappa}$	unit vector in z direction
κ	variational parameter in $f(r)$
κ	Boltzmann's constant (appears only in eq. (26))
κ	compressibility (appears only in eq. (25))
ν	two-body interaction potential
π	angle equal to 180°
σ	distance at which Lennard-Jones potential is zero
ϕ	spherical coordinate

$\phi(r)$ single particle wave function

ψ total wave function

ψ^* complex conjugate of total wave function

$d\Omega_\lambda$ element of solid angle for the λ^{th} molecule

Subscripts:

0 ground state

1 sometimes associated with the λ^{th} molecule

2 sometimes associated with the λ^{th} molecule

i

j

ℓ

s

κ

λ

ρ

Special symbol:

$\langle\,\rangle$ expectation value

APPENDIX B

DETAILS OF MONTE CARLO INTEGRATION

In evaluating equation (17) it is first necessary to calculate the magnitudes of the following vectors $\bar{r}_\kappa - \bar{R}_\kappa$, $\bar{r}_\lambda - \bar{R}_\lambda$, $\bar{r}_\lambda - \bar{r}_\kappa$, $\bar{r}_\kappa - \bar{R}_s$, and $\bar{r}_\lambda - \bar{R}_\rho$ for all sites s and ρ necessary in $\prod_{s\neq\lambda,\kappa} f^2(\bar{r}_\kappa - \bar{R}_s) \prod_{\rho\neq\lambda,\kappa} f^2(\bar{r}_\lambda - \bar{R}_\rho)$ and for all the (λ,κ) pairs evaluated in the summation. This is done for both b.c.c. and f.c.c. lattices.

First we will introduce two new vectors r and z as follows:

$$\bar{r} = \bar{r}_\kappa - \bar{R}_\kappa \tag{B1}$$

$$\bar{z} = \bar{r}_\lambda - \bar{R}_\lambda \tag{B2}$$

Substituting in the other vectors gives

$$\bar{r}_\kappa - \bar{R}_s = \bar{r} + \bar{R}_{\kappa s} \tag{B3}$$

$$\bar{r}_\lambda - \bar{R}_\rho = \bar{z} + \bar{R}_{\lambda\rho} \tag{B4}$$

$$\bar{r}_{\lambda\kappa} = \bar{r}_\lambda - \bar{r}_\kappa = \bar{z} - \bar{r} - \bar{R}_{\kappa\lambda} \tag{B5}$$

Further let us use the notation that $R_o = |R_{\lambda\kappa}|$ when (λ,κ) are nearest neighbors, $R_1 = |R_{\lambda\kappa}|$ when (λ,κ) are second nearest neighbors, etc.

First writing $\bar{r}$ and $\bar{z}$ in Cartesian coordinates gives

$$\bar{z} = z \sin\theta_1 \cos\phi_1 \hat{i} + z \sin\theta_1 \sin\phi_1 \hat{j} + z \cos\theta_1 \hat{\kappa}, \qquad z = |\bar{z}| \tag{B6}$$

$$\bar{r} = r \sin\theta_2 \cos\phi_2 \hat{i} + r \sin\theta_2 \sin\phi_2 \hat{j} + r \cos\theta_2 \hat{\kappa}, \qquad r = |\bar{r}| \tag{B7}$$

With these we can get the magnitudes of the vectors in terms of the six variables r, z, θ_1, θ_2, ϕ_1, ϕ_2. The magnitudes of typical $\bar{r}_\kappa - \bar{R}_s$ and $\bar{r}_\lambda - \bar{R}_\rho$ used in this study are shown in Table BI for a b.c.c. lattice and Table BII for a f.c.c. lattice. Table BIII contains typical $|\bar{r}_{\lambda\kappa}|$'s for both lattices. For the later formulation which involved allowing the nearest neighbors of λ and κ to also move we have

$$\bar{y} \equiv \bar{r}_s - \bar{R}_s = \bar{r}_\rho - \bar{R}_\rho .$$

The vectors $\bar{r}_\kappa - \bar{r}_s$ and $\bar{r}_\lambda - \bar{r}_\rho$ for this case are similar to those in Table BIII.

The calculation of equation (17) for a set of variational parameters β and κ involved evaluating the necessary integrals using standard Monte Carlo techniques.[22] This first step involved changing the variables of integration so that they ranged from $0 \to 1$. Since the integrations over r, y, and z ranged from $0 \to \infty$ these integrations were either cut off at a value $10\ R_o$ when step function biasing was used or left as integrals between $0 \to \infty$ when some form of exponential biasing was used. Biasing of the angular variables had very little effect and therefore was not used for these variables.

The procedure used was to pick a point in six-dimensional (or nine-dimensional) phase space and then use this same point for a trial evaluation of each of the necessary integrals. The $\langle v(r_{ij})\rangle$ and $\left\langle -\frac{h^2}{2m} \nabla^2_{ij} \ln f(r_{ij})\right\rangle$ were evaluated separately. The contribution from each nearest neighbor shell involved three separate integrals: one for $\langle v(r_{ij})\rangle$; another for $\left\langle -\frac{h^2}{2m} \nabla^2_{ij} \ln f(r_{ij})\right\rangle$; and finally a normalization integral. Usually the integrals for the third through the tenth nearest neighbor shells were evaluated together since the normalization integral was nearly identical for each. Since the contributions from these shells are also quite small the effect of this approximation on the potential energy was always less than 0.5 percent and on the kinetic energy less than 0.1 percent.

An exit was made to a statistics subroutine after each set of N points in phase space. The program continued until either a set of criteria on statistics were met or a given number of points in phase space had been evaluated. Typically N ranged from 500 to 1000 and the total number of points from 20 000 to 300 000.

TABLE BI. - MAGNITUDES OF $\overline{r}_\kappa - \overline{R}_s$ AND $\overline{r}_\lambda - \overline{R}_\rho$ FOR A B.C.C. LATTICE

$$|\overline{r}_\kappa - \overline{R}_s|$$

$$[r^2 + R_0^2 + \frac{2rR_0}{\sqrt{3}} (\sin \theta_2 \cos \phi_2 + \sin \theta_2 \sin \phi_2 + \cos \theta_2)]^{1/2}$$

$$[r^2 + R_0^2 + \frac{2rR_0}{3} (-\sin \theta_2 \cos \phi_2 + \sin \theta_2 \sin \phi_2 + \cos \theta_2)]^{1/2}$$

$$[r^2 + R_1^2 + 2rR_1 \sin \theta_2 \cos \phi_2]^{1/2}$$

$$[r^2 + R_1^2 + 2rR_1 \sin \theta_2 \sin \phi_2]^{1/2}$$

$$[r^2 + R_2^2 + \sqrt{2}\, rR_2(\sin \theta_2 \cos \phi_2 + \sin \theta_2 \sin \phi_2)]^{1/2}$$

$$[r^2 + R_2^2 + \sqrt{2}\, rR_2(\sin \theta_2 \cos \phi_2 + \cos \theta_2)]^{1/2}$$

$$|\overline{r}_\lambda - \overline{R}_\rho|$$

$$[z^2 + R_0^2 + \frac{2zR_0}{\sqrt{3}} (\sin \theta_1 \cos \phi_1 + \sin \theta_1 \sin \phi_1 + \cos \theta_1)]^{1/2}$$

$$[z^2 + R_0^2 + \frac{2zR_0}{\sqrt{3}} (-\sin \theta_1 \cos \phi_1 + \sin \theta_1 \sin \phi_1 + \cos \theta_1)]^{1/2}$$

$$[z^2 + R_0^2 + 2zR_1 \sin \theta_1 \cos \phi_1]^{1/2}$$

$$[z^2 + R_1^2 + 2zR_1 \sin \theta_1 \sin \phi_1]^{1/2}$$

$$[z^2 + R_2^2 + \sqrt{2}\, zR_2(\sin \theta_1 \cos \phi_1 + \sin \theta_1 \sin \phi_1)]^{1/2}$$

$$[z^2 + R_2^2 + \sqrt{2}\, zR_2(\sin \theta_1 \cos \phi_1 + \cos \theta_1)]^{1/2}$$

TABLE BII. - MAGNITUDES OF $\overline{r}_\kappa - \overline{R}_s$ AND $\overline{r}_\lambda - \overline{R}_\rho$ FOR A F.C.C. LATTICE

$$|\overline{r}_\kappa - \overline{R}_s|$$

$$[r^2 + R_0^2 + \sqrt{2}\, rR_0(\sin\theta_2 \cos\phi_2 + \sin\theta_2 \sin\phi_2)]^{1/2}$$

$$[r^2 + R_0^2 + \sqrt{2}\, rR_0(\sin\theta_2 \sin\phi_2 + \cos\theta_2)]^{1/2}$$

$$[r^2 + R_1^2 + 2rR_1 \sin\theta_2 \cos\phi_2]^{1/2}$$

$$[r^2 + R_1^2 + 2rR_1 \sin\theta_2 \sin\phi_2]^{1/2}$$

$$|\overline{r}_\lambda - \overline{R}_\rho|$$

$$[z^2 + R_0^2 + \sqrt{2}\, zR_0(\sin\theta_1 \cos\phi_1 + \sin\theta_1 \sin\phi_1)]^{1/2}$$

$$[z^2 + R_0^2 + \sqrt{2}\, zR_0(\sin\theta_1 \sin\phi_1 + \cos\theta_1)]^{1/2}$$

$$[z^2 + R_1^2 + 2zR_1 \sin\theta_1 \cos\phi_1]^{1/2}$$

$$[z^2 + R_1^2 + 2zR_1 \sin\theta_1 \sin\phi_1]^{1/2}$$

TABLE BIII. - MAGNITUDES OF $\bar{r}_{\lambda\kappa}$ FOR A F.C.C. AND B.C.C. LATTICE

b.c.c., $|\bar{r}_{\lambda\kappa}|$

Nearest neighbor pair

1st

$$\Big[z^2 + r^2 + R_0^2 - 2zr(\sin\theta_1 \sin\theta_2 \cos(\phi_1 - \phi_2) + \cos\theta_1 \cos\theta_2) - \frac{2zR_0}{\sqrt{3}} (\sin\theta_1 \cos\phi_1 + \sin\theta_1 \sin\phi_1 + \cos\theta_1) + \frac{2rR_0}{\sqrt{3}} (\sin\theta_2 \cos\phi_2 + \sin\theta_2 \sin\phi_2 + \cos\theta_2)\Big]^{1/2}$$

2nd

$$\Big[z^2 + r^2 + R_1^2 - 2zr(\sin\theta_1 \sin\theta_2 \cos(\phi_1 - \phi_2) + \cos\theta_1 \cos\theta_2) - 2zR_1 \cos\theta_1 + 2rR_1 \cos\theta_2\Big]^{1/2}$$

f.c.c., $|\bar{r}_{\lambda\kappa}|$

1st

$$\Big[z^2 + r^2 + R_0^2 - 2zr(\sin\theta_1 \sin\theta_2 \cos(\phi_1 - \phi_2) + \cos\theta_1 \cos\theta_2 - \sqrt{2}\, zR_0(\sin\theta_1 \cos\phi_1 + \sin\theta_1 \sin\phi_1) + \sqrt{2}\, rR_0(\sin\theta_2 \cos\phi_2 + \sin\theta_2 \sin\phi_2)\Big]^{1/2}$$

2nd

$$\Big[z^2 + r^2 + R_1^2 - 2zr(\sin\theta_1 \sin\theta_2 \cos(\phi_1 - \phi_2) + \cos\theta_1 \cos\theta_2) - 2zR_1 \sin\theta_1 \cos\phi_1 + 2rR_1 \sin\theta_2 \cos\phi_2)\Big]^{1/2}$$